Biodegradation by bacteria in clouds: An underestimated sink for some organics in the atmospheric multiphase system

Amina Khaled[1], Minghui Zhang[1], Pierre Amato[1], Anne-Marie Delort[1], and Barbara Ervens[1]

[1]Université Clermont Auvergne, CNRS, SIGMA Clermont, Institut de Chimie de Clermont-Ferrand, 63000 Clermont-Ferrand, France

Corresponding author: Amina.Khaled@uca.fr

Abstract. Water-soluble organic compounds represent a significant fraction of total atmospheric carbon. The main oxidants towards them in the gas and aqueous phases are OH and NO_3 radicals. In addition to chemical solutes, a great variety of microorganisms (e.g. bacteria, viruses, fungi) has been identified in cloud water. Previous lab studies suggested that for some organics, biodegradation by bacteria in water is comparable to their loss by chemical processes. We perform model sensitivity studies over large ranges of biological and chemical process parameters using a box model with a detailed atmospheric multiphase chemical mechanism and biodegradation processes to explore the importance of biodegradation of organics in the aqueous phase. Accounting for the fact that only a small number fraction of cloud droplets (~0.0001 – 0.001) contains active bacteria cells, we consider only a few bacteria-containing droplets in the model cloud. We demonstrate that biodegradation might be most efficient for water-soluble organic gases with intermediate solubility (~$10^4 \leq K_{H(eff)}$ [M atm^{-1}] $\leq 10^6$, e.g., formic and acetic acids). This can be explained by the transport limitation due evaporation of organics from bacteria-free droplets to the gas phase, followed by the dissolution into bacteria-containing droplets. For CCN-derived compounds, such as dicarboxylic acids, the upper limit of organic loss by biodegradation can be approximated by the amount of organics dissolved in the bacteria-containing droplets ($< 0.1\%$). We compare results from our detailed drop-resolved model to simplified model approaches, in which (i) either all cloud droplets are assumed to contain the same cell concentration (0.0001 – 0.001 cell droplet^{-1}), or (ii) only droplets with intact bacteria cells are considered in the cloud (liquid water content ~10^{-11} vol/vol). Conclusions based on these approaches generally overestimate the role of biodegradation, in particular, for highly water-soluble organic gases. Our model sensitivity studies suggest that current atmospheric multiphase chemistry models are incomplete for organics with intermediate solubility and high bacterial activity.

1. Introduction

Clouds provide a medium for multiphase chemical reactions, in which chemical species from the aqueous, solid and gas phases are transformed and can affect significantly the transport and distribution of chemical species in the atmosphere (Lelieveld and Crutzen, 1991). The chemical composition of cloud water is a complex mixture containing a multitude of organic and inorganic species with a range of chemical and physical properties (e.g., reactivity, solubility, volatility). The organic fraction includes water-soluble organic gases and water-soluble CCN-derived components, such as aldehydes, mono- and dicarboxylic acids, organonitrogen and organosulfur compounds. Water-soluble organic gases are dissolved from the gas phase to the aqueous phase; CCN-derived compounds enter the aqueous phase via nucleation scavenging of condensation nuclei (CCN) (Ervens, 2015; Löflund et al., 2002). Water-soluble organic carbon (WSOC) constitutes a significant portion of the total atmospheric organic carbon mass, ranging from ~14% to ~64% depending on the sampling location (Decesari et al., 2000; Gao et al., 2016; Varga et al., 2001).

In addition to chemical solutes, cloud water contains microorganisms such as bacteria, yeast and fungi (Delort et al., 2010; Hu et al., 2018). Typical concentrations of bacteria cells are on the order of 10^6 to 10^8 cells L^{-1}; fungi and yeast cell concentrations are usually lower (~10^5 to ~10^7 cells L^{-1}) (Amato et al., 2007c; Sattler et al., 2001). The atmosphere is a stressful environment for microorganisms (low temperature, UV exposure, acidic pH, quick hydration/drying cycles and the presence of oxidants such as OH, H_2O_2) (Sattler et al., 2001), which might limit the survival time of cells in the atmosphere.

Several studies have shown that bacteria can grow and be metabolically active in cloud droplets. Marker compounds such as adenosine 5'-triphosphate (ATP) (Amato et al., 2007d), rRNA (Krumins et al., 2014a) or mRNA (Amato et al., 2019) have been used to demonstrate metabolic activity in the atmosphere. The ADP/ATP ratio, monitored during lab experiments with real cloud water, showed that even after exposure to oxidants over several hours, biodegradation rates were not significantly affected (Vaïtilingom et al., 2013a). Metabolic activity and cell generation of bacteria is likely restricted to the time cells spent in clouds due to the abundance of liquid water (Ervens and Amato, 2020; Haddrell and Thomas, 2017); bacteria have been found to be dormant at lower relative humidity than in clouds (Kaprelyants and Kell, 1993).

The metabolic activity of bacterial strains identified in cloud water (e.g. *Pseudomonas, Sphingomonas*) has been investigated in lab studies, and it was shown that they can biodegrade organics (e.g., malonate, succinate, adipate, pimelate, formaldehyde, methanol, acetate, formate, phenol and catechol) (Amato et al., 2007b; Ariya et al., 2002; Delort et al., 2010; Fankhauser et al., 2019; Husárová et al., 2011; Jaber et al., 2020; Vaïtilingom et al., 2010a, 2011, 2013b). Based on comparisons of experimentally derived biodegradation rates to chemical rates of oxidation reactions by radicals (e.g., OH, NO_3) in the aqueous phase, it was concluded that they might be similar under some conditions, and that, depending on the abundance and metabolic activity of bacteria strains, oxidation and biodegradation processes of organics

may compete in clouds. The biodegradation rate likely depends on the availability of the substrate in the aqueous phase. In the case of soluble substrates, it can be expected that uptake of soluble substrates from the gas phase leads to a continuous replenishment of the organics.

There are several estimates of WSOC loss by bacteria on a global scale: Sattler et al. (2001) estimated a sink of 1- 10 Tg yr^{-1}, smaller than the estimate by (Vaïtilingom et al., 2013) (10-50 Tg yr^{-1}). However, the latter is likely an overestimate as complete respiration was implied, i.e. total conversion of organics into CO_2. More conservatively, Ervens and Amato (2020) suggested a global WSOC loss of 8–11 Tg yr^{-1}, being comparable to that by chemical processes (8–20 Tg yr^{-1}). Similarly, Fankhauser et al. (2019) postulated that the role of biodegradation is likely small but they did not quantify the loss of different organics by bacteria.

Current atmospheric multiphase chemistry models include chemical mechanisms of different complexity with up to thousands of chemical reactions describing the transformation of inorganic and organic compounds, e.g. (Ervens et al., 2003a; Mouchel-Vallon et al., 2017; Tilgner et al., 2013; Woo and McNeill, 2015). However, they do not include the biodegradation of organics by bacteria despite the available data sets discussed above.

Cloud chemistry models often assume initially identical composition of all cloud droplets. While this might be a reasonable assumption for the chemical droplet composition due to internally mixed CCN and the phase transfer from the gas phase into all droplets, it is not appropriate for the distribution of bacteria. Due to their small number fraction of the total CCN concentration (0.001 – 0.1 %, e.g.,(Zhang et al., 2020), the fraction of cloud droplets that contain bacteria cells is small (< 0.001). Thus, to explore biodegradation of organics in the atmospheric multiphase system, a realistic distribution within cloud droplet population needs to be assumed.

The aim of our study is to identify conditions, under which biodegradation in clouds is significant in the atmosphere. Using a cloud multiphase box model, we explore the biological and chemical degradation of organic compounds over large parameter ranges of biodegradation activities, chemical rate constants and Henry's law constants. We compare (1) the biodegradation rates in the aqueous phase to the chemical rates in both phases, and (2) the fraction of organics consumed by biodegradation to that by chemical processes. The results of our sensitivity studies elucidate, for which organics biodegradation competes with chemical processes. Our study will give guidance for future experimental and modeling studies to further complete atmospheric models in order to more comprehensively describe organic degradation in the atmosphere.

2.   Methods

2.1   Description of the multiphase box model

We use a multiphase box model with detailed gas and aqueous phase chemistry (75 species, 44 gas phase reactions, 31 aqueous reactions (Ervens et al., 2008).

The chemical aqueous phase mechanism with rate constants is listed in **Table S1.** The chemical gas phase
100   mechanism is based on the NCAR Master mechanism (Aumont et al., 2000; Madronich and Calvert, 1989).
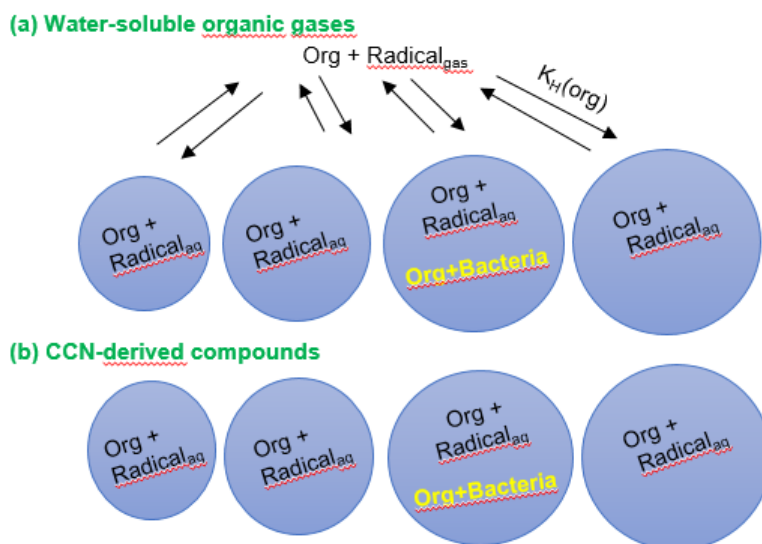
Figure 1: Schematic of the multiphase box model including chemical radical reactions in the gas and
aqueous phases. Chemical reactions occur in both phases and in all droplets whereas
biodegradation processes only occur in the aqueous phase in a small fraction of droplets,
depending on the assumed bacteria cell concentration in clouds. (a) water-soluble organic
gases that partition between the two phases (b) CCN-derived compounds that get only
processed in the aqueous phase.

The two phases are coupled by 26 phase transfer processes which is described kinetically based on the
resistance model by Schwartz (1986). The parameters describing the phase transfer of the soluble species
are presented in **Table S2**. In addition, the initial mixing ratios of gas phase species are included in **Table**
105   **S3**. The equations for the mass transfer coefficient k_{mt} and the differential equations for the aqueous and gas
phase concentrations can be found in the supplement (**Eq-R1-R3**; Section 'Description of phase transfer')
(Seinfeld and Pandis, 1998). In addition to the base chemical mechanism, we define one organic species
'Org' that undergoes chemical radical reactions in the gas and aqueous phases and biodegradation by
bacteria only in the aqueous phase in a small subset of the droplets as shown in **Figure 1**. We consider a
110   polydisperse droplet population of 263 droplets cm^{-3} in 11 size classes with drop diameters of 5 µm $\leq D_{droplet}$
$\leq$ 30 µm and a total liquid water content of LWC = 6.8×10^{-7} vol/vol. Only one droplet size class includes
bacteria cells ($D_{droplet}$ = 20 µm; $N_{droplet}$ = cell concentration = 0.01 cm(gas)$^{-3}$). Thus, the cell concentration in
the cloud water (C_{cell}= 1.5×10^{7} cell L(aq)$^{-1}$) is similar to that found in ambient clouds and as used in lab
experiments (Vaïtilingom et al., 2013b). The model simulations are performed for 600s which corresponds
115   approximately to the droplet lifetime during one cloud cycle (Ervens et al., 2004).

We categorize four various compounds groups bases on their solubility in water and their Henry's law constant and we distinguish:

1) Low-solubility species with $K_H < 10^3$ M atm^{-1}. Their dissolved fraction is < 1% for the liquid water content (LWC) of 0.68 g m^{-3} in our model.

120   2) Intermediate solubility species with 10^3 M atm^{-1} < K_H < 10^6 M atm^{-1} with dissolved fractions of ~1 - 58% (LWC = 0.68 g m^{-3})

3) High-solubility species with $K_H > 10^6$ M atm^{-1} for which the dissolved fraction exceeds 95 % (LWC = 0.68 g m^{-3}).

4) Water-soluble CCN components which are dissolved in the aqueous phase upon dissolution of the
125   condensation nucleus on which the cloud droplet grew. While these compounds have usually low volatility or are semi-volatile, they also need to be water-soluble to be available for aqueous phase processes.

2.2   Kinetic data in the gas and aqueous phases

2.2.1   Chemical rates and Henry's law constants

Table 1 includes chemical rate constants for radical (OH, NO$_3$) reactions in the aqueous and gas phases for
130   organic compounds, for which lab data on their biodegradation rates are available (*Section 2.2.2*). This data covers ranges of $10^3 \leq k_{chemaq}$ [M^{-1} s^{-1}] $\leq 10^{10}$ and $10^{-17} \leq k_{chemgas}$ [cm^3 s^{-1}] $\leq 10^{-10}$, respectively, over which the model sensitivity studies in the following are performed.

Table 1. Literature data on chemical rate constants in the aqueous ($k_{OH,aq}$; $k_{NO3,aq}$) and gas phases ($k_{OH,gas}$; $k_{NO3,gas}$) , physical Henry's law constants (K_H) and effective Henry's law constants ($K_{H(eff)}$) for
135   acids at pH = 3 and pH = 6 respectively.

Organic compounds	$k_{OH,aq}$ (25°C) [M^{-1} s^{-1}]	$k_{OH,gas}$ (25°C) [cm^3 s^{-1}]	$k_{NO3,aq}$ [M^{-1} s^{-1}]	$k_{NO3,gas}$ [cm^3 s^{-1}]	K_H [M atm^{-1}]	pK$_a$	$K_{H(eff)}$ [M atm^{-1}] at pH = 3, pH = 6
CCN-derived compounds							
Malonic acid	1.6 ×10^7 (1)		5.1×10^4 (1)				
Malonate monoanion	3.6×10^8 (1)		5.6×10^6 (1) 2.3×10^7 (1)		1.23×10^{10} (12)	2.8 5.6	3.18×10^{10} 6.84×10^{13}
Malonate dianion	8.0×10^7 (1)						
Succinic acid	3.8×10^8 (2)		5×10^3 (1)		3.5×10^9 (12)	4.23 5.64	3.70×10^{10} 6.81×10^{11}
Succinate monoanion	5×10^8 (1)		1.1×10^7 (1) 1.8×10^7 (1)				

Succinate dianion	5×10^8 (5)						
Water-soluble organic gases							
Acetic acid	1.6×10^7 (3)	6.6×10^{-13} (6)	1.3×10^4 (8)	-	7×10^3 (13)	4.75	7.1×10^3 1.3×10^5
Acetate	8.5×10^7 (1)		2.3×0^6 (8)				
Formic acid	1.3×10^8 (3)	1.3×10^{-12} (7)	3.3×10^4 (1)	-	11×10^3 (13)	3.76	1.2×10^4 1.9×10^6
Formate	3.2×10^9 (1)		4.2×10^7 (1)			-	-
Formaldehyde	6.1·10^8 (1)	8.5×10^{-12} (1)	7.9×10^5 (11)		3×10^3 (14)	-	-
Catechol	3.8·10^8 (4)	1×10^{-12} (5)	8.4×10^9 (9)		8.3×10^5 (4)	-	-
Phenol	1.9·10^9 (1)	1×10^{-12} (5)	1.9×10^9 (1)	5.8·10^{-12}	6.47×10^2 (4)	-	-
Methanol	8.7·10^8 (1)	7.7×10^{-13} (1)	2.07×10^5 (10)	-	2.9×10^2 (12)	-	-

(1)(Herrmann, 2003); (2) (Cabelli et al 1985); (3)(Vaïtilingom et al., 2010a); (4) (Pillar et al., 2014) (5) (Ervens et al., 2003c) ;(6)(Butkovskaya et al., 2004); (7)(Anglada, 2004); (8)(Exner et al., 1994); (9)(Hoffmann et al., 2018); (10) (Mezyk et al., 2017); (11)(Gaillard De Sémainville et al., 2007); (12) (Sander, 2015); (13) (Johnson et al., 1996); (14)(Allou et al., 2011); (-): no rate constant available.

In order to generalize our results for different radical concentrations, we present them in terms of chemical rates R_{chem} [s^{-1}] i.e. as the products of the rate constants k_{chemaq} and $k_{chemgas}$ and radical concentrations:

$$R_{chemaq}[s^{-1}] = \frac{-d(org)_{radical}}{dt} = k_{chemaq}[L\ mol^{-1}\ s^{-1}] \times [radical]_{aq}\ [mol\ L^{-1}] \qquad \text{Eq- 1}$$

$$R_{chemgas}[s^{-1}] = \frac{-d(org)_{radical}}{dt} = k_{chemgas}[cm^3\ s^{-1}] \times [radical]_{gas}\ [cm^{-3}] \qquad \text{Eq- 2}$$

Typical radical concentrations are on the order of 10^{-15} mol L^{-1} for OH and NO$_3$ radicals in the aqueous phase of clouds (Arakaki et al., 2013; Herrmann, 2003) and 10^6 cm^{-3} and 10^7 - 10^8 cm^{-3} in the gas phase, respectively (Cantrell et al., 1997; Khan et al., 2008). The Henry's law constants for the same organic compounds are also listed *Table 1*. They cover a range of 10$^2 \le K_H$ [M atm^{-1}] $\le$ 10^9. For carboxylic acids, we also report effective Henry's law constants at pH = 3 and pH = 6 as being typical for cloud water.

2.2.2   Biodegradation rates

In the literature, experimental rates for metabolic processes are usually reported in units of [mol cell^{-1} s^{-1}] (*Table 2*). We converted these rates into first order loss rates k$^{1st}_{bact}$ [s^{-1}] by dividing them by the ratio of the concentration of the organic compound [mol L^{-1}] to C$_{cell,aq}$ [cell L^{-1}] used in the respective experiments. To obtain a value with units corresponding to chemical rate constants, this rate is divided by the constant model cell concentration (C$_{cell,aq}$ = 1.5×10^7 cell L^{-1}) resulting in a range of 10$^{-18} \le$ k$_{bact}$ [L cell^{-1} s^{-1}] $\le$ 10^{-11}. This cell concentration is on the same order of magnitude as found in many clouds (Amato et al., 2007d).

Experiments with 17 different cloud bacteria in artificial cloud water with pH = 5.0 and pH = 6.5 showed

also nearly identical results (Vaïtilingom et al., 2011). Similar results were shown by Razika et al. (2010) who demonstrated that biodegradation rates of phenol by *Pseudomonas aeruginosa* were very similar when incubated at pH = 5.8, 7.0 and 8.0, respectively. When exposed to very broad ranges of external pHs, bacteria can control their intracellular pH (~6.5 -7) by internal buffering (Delort et al., 2017). As biodegradation occurs inside the cell, it takes place at these (nearly) neutral conditions. The efficiency of buffering decreases at extreme conditions, e.g., pH < 2 or pH > 10 (Guan and Liu, 2020). However, such pH range is not representative for cloud water where more moderate pH values (~ 3 – 6) are typically found (Deguillaume et al., 2014). Therefore, we do not consider a potential pH dependency of biodegradation rates in our model studies.

Similar to the chemical processes (Eqs 1 and 2), we express the biological activity in terms of a rate

$$R_{bact}[s^{-1}] = \frac{-d(org)_{bact}}{dt} = k_{bact}[\,L\;Cell^{-1}s^{-1}] \times C_{cell,aq}[Cell\;L^{-1}] \qquad \text{Eq- 3}$$

whereas k_{bact} is the bacterial rate constant [L cell^{-1} s^{-1}] and $C_{cell,aq}$ is the concentration of bacteria in cloud water [cell L^{-1}].

Table 2. Summary of biodegradation rates from the literature and calculated rate constants (k_{bact}) for the consumption of small organic species by bacteria isolated from cloud water.

Organic compound	Bacteria type	Concentration in the experiments		Experimental rate [mol cell^{-1} s^{-1}]		Calculated k$^{1st}_{bact}$ [s^{-1}]		Calculated k$_{bact}$ [cell^{-1} L s^{-1}]		Ref
		Cells [cell mL^{-1}]	Organic [mol L^{-1}]	17°C	5°C	17°C	5°C	17°C	5°C	
Form-aldehyde	*P graminis*	8×10^4	0.02	1.9×10^{-20}	8.1×10^{-21}	7.7×10^{-11}	3.2×10^{-11}	4.8×10^{-18}	2.1×10^{-18}	1
	Pseudomonas sp.			1.4×10^{-19}	8.6×10^{-20}	5.6×10^{-10}	3.4×10^{-10}	3.7×10^{-17}	2.3×10^{-17}	
	Frigoribacterium sp.			6.4×10^{-21}	6.4×10^{-21}	2.6×10^{-11}	2.6×10^{-11}	1.7×10^{-18}	1.7×10^{-18}	
	Bacillus sp.			2.0×10^{-20}	3.1×10^{-21}	8.1×10^{-11}	1.2×10^{-11}	5.4×10^{-18}	8.4×10^{-19}	
Formate	*Sphingomonas* sp.	10^9	0.02	9.2×10^{-21}	3.1×10^{-20}	4.6×10^{-7}	1.6×10^{-6}	3.0×10^{-14}	$1.0x\times0^{-13}$	2
	P graminis			1.3×10^{-19}	9.6×10^{-20}	6.5×10^{-6}	4.8×10^{-6}	4.3×10^{-13}	3.2×10^{-13}	
	Pseudomonas sp.			4.6×10^{-20}	8.6×10^{-21}	2.3×10^{-6}	4.3×10^{-7}	1.5×10^{-13}	2.8×10^{-14}	
	P viridiflava			1.6×10^{-19}	4.7×10^{-20}	8.1×10^{-6}	2.3×10^{-6}	5.4×10^{-13}	1.5×10^{-13}	
	Rhodococcus sp.	10^6	2×10^{-5}	8.0×10^{-19}	4.0×10^{-19}	4.0×10^{-5}	2.0×10^{-5}	2.6×10^{-12}	1.3×10^{-12}	3
	Pseudomonas sp.			1.5×10^{-18}	8.0×10^{-19}	7.5×10^{-6}	4.0×10^{-5}	5.0×10^{-13}	3.4×10^{-13}	
	P syringae			2.3×10^{-18}	2.0×10^{-18}	1.1×10^{-4}	1.0×10^{-4}	7.3×10^{-12}	6.6×10^{-12}	
	P graminis			5.0×10^{-18}	1.0×10^{-18}	2.5×10^{-4}	5.0×10^{-5}	1.6×10^{-11}	3.3×10^{-12}	
	Various microorganisms	8×10^4	43×10^{-6}	2.1×10^{-18}		4.1×10^{-6}		2.7×10^{-13}		4
Acetate	*Sphingomonas* sp.	10^9	0.02	2.7×10^{-20}	1.6×10^{-22}	1.3×10^{-6}	8.2×10^{-9}	1.1×10^{-13}	5.4×10^{-16}	2
	P graminis			3.0×10^{-19}	3.0×10^{-20}	1.5×10^{-5}	1.5×10^{-6}	1.0×10^{-12}	1.0×10^{-13}	
	Pseudomonas sp.			2.6×10^{-20}	1.7×10^{-20}	1.3×10^{-6}	8.8×10^{-7}	8.7×10^{-14}	5.3×10^{-14}	
	P viridiflava			5.6×10^{-20}	1.1×10^{-20}	2.8×10^{-6}	6.0×10^{-7}	1.8×10^{-13}	4.0×10^{-14}	
	Rhodococcus sp.	10^6	2×10^{-5}	5.0×10^{-18}	1.0×10^{-18}	2.5×10^{-4}	5.0×10^{-5}	1.6×10^{-11}	3.3×10^{-12}	3
	Pseudomonas sp.			1.3×10^{-18}	6.0×10^{-19}	6.7×10^{-5}	3.0×10^{-5}	4.5×10^{-12}	2.0×10^{-12}	
	P syringae			8.6×10^{-19}	2.0×10^{-19}	4.3×10^{-5}	1.0×10^{-5}	2.8×10^{-12}	6.6×10^{-13}	
	P graminis			4.0×10^{-19}	1.0×10^{-19}	2.0×10^{-5}	5.0×10^{-6}	1.3×10^{-12}	3.3×10^{-13}	
	Various microorganisms	8×10^4	2.5×10^{-6}	1.94×10^{-18}		6.25×10^{-3}		4.16×10^{-10}		4
Succinate	*Sphingomonas* sp.	10^9	0.02	2.6×10^{-20}	1.0×10^{-20}	1.3×10^{-6}	5.4×10^{-7}	8.6×10^{-14}	3.6×10^{-14}	2
	P graminis			1.0×10^{-19}	9.8×10^{-20}	5.2×10^{-6}	4.9×10^{-6}	3.4×10^{-13}	3.2×10^{-13}	
	Pseudomonas sp.			1.4×10^{-20}	1.8×10^{-20}	7.0×10^{-7}	9.2×10^{-7}	4.7×10^{-14}	6.1×10^{-14}	
	P viridiflava			2.9×10^{-20}	6.1×10^{-20}	1.4×10^{-6}	3.0×10^{-6}	9.7×10^{-14}	2.0×10^{-13}	
	Rhodococcus sp.	10^6	2×10^{-5}	5.0×10^{-20}	4.0×10^{-20}	2.5×10^{-6}	2.0×10^{-6}	1.6×10^{-13}	1.3×10^{-13}	3
	Pseudomonas sp.			1.5×10^{-19}	2.0×10^{-20}	7.5×10^{-6}	1.0×10^{-6}	5.0×10^{-13}	6.6×10^{-14}	
	P syringae			6.8×10^{-19}	1.7×10^{-19}	3.4×10^{-5}	8.8×10^{-6}	2.2×10^{-12}	5.8×10^{-13}	
	P graminis			5.0×10^{-19}	1.0×10^{-19}	2.5×10^{-5}	5.0×10^{-6}	1.6×10^{-12}	3.3×10^{-13}	
	Various microorganisms	8×10^4	3.1×10^{-6}	5.6×10^{-19}		1.4×10^{-5}		9.6×10^{-13}		4
Malonate	Various microorganisms	8×10^4	3.1×10^{-6}	5.2×10^{-19}		1.3×10^{-5}		9.0×10^{-13}		4
Catechol	*R enclensis*	10^7	0.0001	4.1×10^{-19}		4.1×10^{-8}		2.7×10^{-15}		5
Phenol	*R enclensis*	10^9	0.0001	5.0×10^{-20}		5.0×10^{-4}		3.3×10^{-11}		5
Methanol	*P graminis*	8×10^4	0.02	5.6×10^{-22}	-	2.2×10^{-12}	-	1.5×10^{-19}	0	1
	P syringae			5.7×10^{-21}	5.8×10^{-22}	2.3×10^{-11}	2.3×10^{-12}	1.5×10^{-18}	1.5×10^{-19}	
	Frigoribacterium sp.			3.5×10^{-23}	2.5×10^{-23}	1.4×10^{-13}	1.0×10^{-13}	9.4×10^{-21}	6.7×10^{-21}	
	Bacillus sp.			2.9×10^{-21}	-	1.1×10^{-11}	-	7.8×10^{-19}	0	

(1)(Husárová et al., 2011); (2)(Vaïtilingom et al., 2010a); (3)(Vaïtilingom et al., 2011); (4)(Vaïtilingom et al., 2013b); (5)(Jaber et al., 2020). Several experiments showed that temperature only had a small influence on the biodegradation rates that differed at most by a factor of 2 in experiments at 5°C or 17°C (Husárová et al., 2011; Vaïtilingom et al., 2010a, 2011).

2.3 Definition of model output parameters

2.3.1 Relative contributions to biodegradation and chemical loss rates

Several previous studies compared biodegradation and chemical rates in order to conclude on the potential importance of biological processes in clouds (Ariya et al., 2002; Husárová et al., 2011; Jaber et al., 2020; Vaïtilingom et al., 2011, 2013b). Similarly, we define the relative contributions of the bacterial and the chemical processes in the two phases to the total loss rate of an organic compound

$$R'_{bact}[mol\ L^{-1}s^{-1}] = R_{bact}[s^{-1}] \times C_{org,aq}\ [mol\ L^{-1}] \qquad \text{Eq-4}$$

$$R'_{chemaq}[mol\ L^{-1}s^{-1}] = R_{chemaq}[\ s^{-1}] \times C_{org,aq}\ [mol\ L^{-1}] \qquad \text{Eq-5}$$

$$R'_{chemgas}[\ cm^{-3}\ s^{-1}] = R_{chemgas}[\ s^{-1}] \times C_{org,gas}[cm^{-3}] \qquad \text{Eq-6}$$

where $C_{org,aq}$ and $C_{org,gas}$ are the concentration of water-soluble organic gases in the aqueous [mol L^{-1}] and gas phases [cm^{-3}], respectively. Their relative contributions are then expressed as

$$fr_{bact}[\%] = \frac{R'_{bact}}{R'_{bact} + R'_{chemaq} + R'_{chemgas}} \times 100 \qquad \text{Eq- 7}$$

$$fr_{chemaq}[\%] = \frac{R'_{chemaq}}{R'_{bact} + R'_{chemaq} + R'_{chemgas}} \times 100 \qquad \text{Eq- 8}$$

$$fr_{chemgas}[\%] = \frac{R'_{chemgas}}{R'_{bact} + R'_{chemaq} + R'_{chemgas}} \times 100 \qquad \text{Eq- 9}$$

whereas these fractions always add up to 100%. As CCN-derived compounds are only in the aqueous phase, $fr_{chemgas,CCN-derived} = 0$.

2.3.2 Contributions to total loss of organics by bacterial and chemical processes

While fr_{bact}, fr_{chemaq} and $fr_{chemgas}$ define the relative importance of the bacterial and chemical loss rates, they do not give quantitative information on the total loss of the organics. To define this sink strength, we introduce the parameter L_t [%] as:

$$L_t[\%] = 100 - \left[\frac{[Org]_t}{[Org]_0} \times 100\right] = L_{bact} + L_{chemaq} + L_{chemgas} \qquad \text{Eq-10}$$

whereas [Org]$_0$ is the initial organic concentration (1 ppb) and [Org]$_t$ is the organic concentration at time t (for most simulations: t = 600s). Accordingly, L_{bact}, $L_{,chemaq}$ and $L_{chemgas}$ are the fractions [%] of organics consumed by bacteria and radicals in the aqueous and gas phases, respectively.

$$L_{bact}[\%] = fr_{bact}[\%] \times L_t[\%] \div 100\% \qquad \text{Eq-11}$$

$$L_{chemaq}[\%] = fr_{chemaq}[\%] \times L_t[\%] \div 100\% \qquad \text{Eq-12}$$

$$L_{chemgas}[\%] = fr_{chemgas}[\%] \times L_t[\%] \div 100\% \qquad \text{Eq-13}$$

As both the fractions 'fr' and L are expressed in percent, we divided by 100% in Equations 11-13. Unlike the sum of fr_{bact}, fr_{chemaq} and $fr_{chemgas}$ that always yields 100% (**Eqs 7- 9**), by definition, L_t does not have to reach 100%. As we only consider one cloud cycle in our simulations (t = 600s), the values of L_t, L_{bact}, $L_{chemgas}$ and L_{chemaq} are rather small (a few percent at most); however, it should be kept in mind that particles likely undergo multiple cloud cycles during their residence time in the atmosphere. Thus, the contribution of chemical and biological processes to the total loss for a specific organic can be extrapolated for longer time scales based on our results. However, as one of the main goals of our study is to compare biodegradation to the better constrained chemical losses, our conclusions will be independent of the time scales.

3. Results and discussion

3.1 Relative loss rate of organics by biological processes (fr_{bact})

3.1.1 fr_{bact} of water-soluble organic gases

We first compare the contributions of biodegradation and chemical losses to the total loss rate for water soluble organic gases. In order to cover a representative parameter range of the physicochemical properties of the organic compound, we performed five simulations, in all of which the full ranges of K_H and of R_{chemaq} over eight orders of magnitude were explored (*Section 2.2*). The simulations differ by the assumptions of $R_{chemgas}$ and R_{bact} that are kept constant in the individual model runs: For the results shown in *Figure 2a, b,* and *c*, we applied $R_{bact} = 10^{-8}$ s^{-1}, 10^{-6} s^{-1} and 10^{-4} s^{-1} and $R_{chemgas} = 10^{-6}$ s^{-1}, respectively. For the three sets of simulations shown in *Figure 2b, d,* and *e*, $R_{bact} = 10^{-6}$ s^{-1} and $R_{chemgas}$ equal to 10^{-6} s^{-1}, 10^{-5} s^{-1} and 10^{-4} s^{-1}, were assumed. Thus, in total three values each for $R_{chemgas}$ and R_{bact} are discussed in the following.

In general, for all combinations of $R_{chemgas}$ and R_{bact}, the highest fr_{bact} is predicted for organics with the highest solubility (K_H [M atm^{-1}] ≥ 10^8) and lowest chemical reaction rate in the aqueous phase (R_{chemaq} [s^{-1}] ≤ 10^{-11}). For the lowest biological activity ($R_{bact} = 10^{-8}$ s^{-1}, *Figure 2a*), fr_{bact} reaches a maximum value of ~100%. For higher biological activity ($R_{bact} = 10^{-6}$ s^{-1} and 10^{-4} s^{-1}), fr_{bact} is always smaller and only reaches at most ~80% (*Figure 2b and 2c*). This trend seems counterintuitive as for the highest R_{bact}, the highest importance of biodegradation may be expected. We will explore the reasons for this further in *Section 3.1.2* where we compare loss rates in individual droplets as a function of time.

The comparison of *Figures 2b* and *2c* shows that the parameter ranges, for which fr_{bact} has the maximum value, are broader for higher R_{bact}: When $R_{bact} = 10^{-6}$ s^{-1} (*Figure 2b*), fr_{bact} ~80% within the ranges of ~10^7 ≤ K_H [M atm^{-1}] ≤ ~10^9 and 10^{-12} ≤ R_{chemaq} [s^{-1}] ≤ 10^{-10}, i.e. both R_{chemaq} and K_H span about two orders of magnitude. For $R_{bact} = 10^{-4}$ s^{-1} (*Figure 2c*), these ranges are ~10^5 ≤ K_H [M atm^{-1}] ≤ ~10^9 and 10^{-12} ≤ R_{chemaq}

s$^{-1}] \leq 10^{-9}$, i.e., wider by about two and one order of magnitude, respectively.
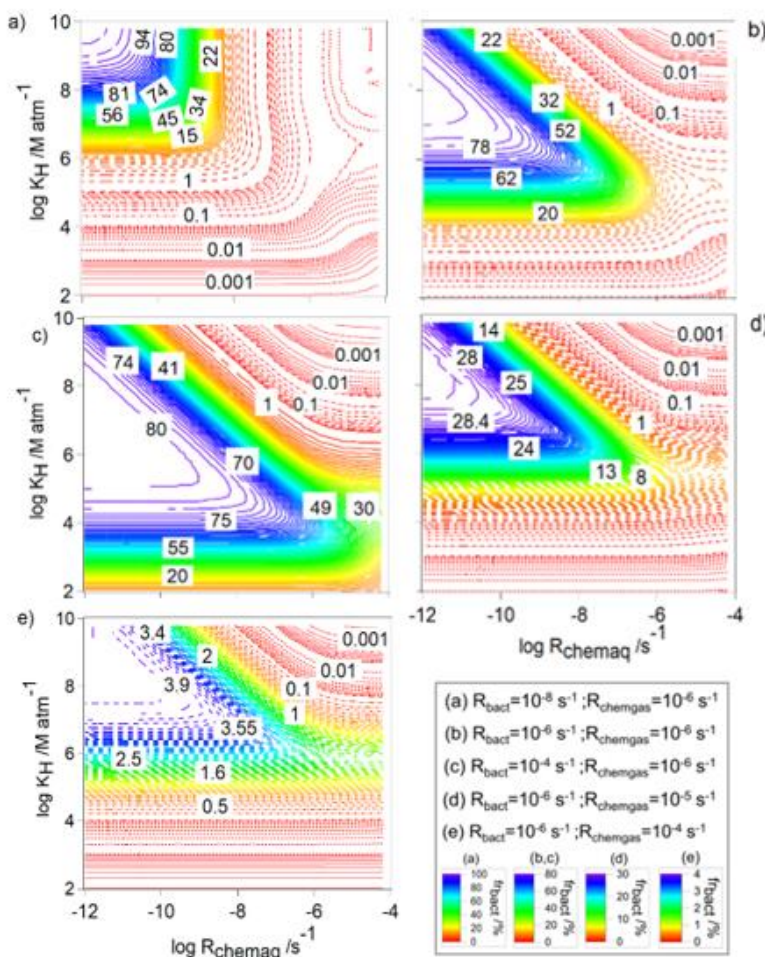
Figure 2. Relative contribution of bacteria to the total loss rate of organics (*fr$_{bact}$*, Eq-7) as a function of R$_{chemaq}$ and K$_H$. All figure panels have the same scales on the ordinates and abscissas, respectively. The simulations were performed for constant values of R$_{bact}$ and R$_{chemgas}$; their values are indicated in the box at the bottom right.

This widening of the parameter spaces can be explained by the contributions of the chemical processes to the total organic loss rate, i.e. fr$_{chemaq}$ and fr$_{chemgas}$ (***Figures S1*** and ***S2*** in the supplement): For the two values of R$_{bact}$, fr$_{chemaq}$ is highest (> 80%) for a combination of (i) ~$10^5 \leq$ K$_H$ [M atm^{-1}] $\leq 10^9$ and ~$10^{-9} \leq$ R$_{chemaq}$ [s$^{-1}] \leq 10^{-5}$, or of (ii) low/intermediate solubility (~$10^3 \leq$ K$_H$ [M atm^{-1}] $\leq$ ~10^5) and high chemical aqueous phase reactivity ($10^{-6} \leq$ R$_{chemaq}$ [s$^{-1}] \leq 10^{-5}$). These trends are due to the predominant partitioning of highly soluble organics to the aqueous phase (> 90% for K$_H \geq 10^6$ M atm^{-1}). If R$_{chemaq}$ is low, the organics do not undergo efficient chemical processes in the aqueous phase. Therefore, fr$_{bact}$ is highest for this parameter combination. The comparison of the results for R$_{bact} = 10^{-6}$ s^{-1} and three values of R$_{chemgas}$ (***Figure 2b, d, e***) shows a decrease of the maximum value of fr$_{bact}$ from 80% (***Figure 2b***) to 4% (***Figure 2e***) for similar ranges of K$_H$ and R$_{chemaq}$ because of the dependence of fr$_{bact}$ on fr$_{chemgas}$: for compounds with highest R$_{chemgas}$, the

dominant loss is the gas phase reaction, leading to a high $fr_{chemgas}$ and consequently to a lower fr_{bact} (***Figure 2e***). Therefore, the parameter ranges of K_H and R_{chemaq}, where fr_{bact} is maximum, do not change for different $R_{chemgas}$, but decrease when the gas phase chemistry dominates the loss of the organic.

Overall, the variation in fr_{bact} as a response to changes in R_{chemaq}, $R_{chemgas}$ and K_H shows different sensitivities: For example, for organics with $K_H = 10^6$ M atm^{-1}, $R_{chemaq} = 10^{-9}$ s^{-1} and $R_{chemgas} = 10^{-6}$ s^{-1}, fr_{bact} is ~8% when $R_{bact} = 10^{-8}$ s^{-1} (red area in ***Figure 2a***). This fraction increases to fr_{bact} ~ 73%, i.e. by a factor of ~9, when $R_{bact} = 10^{-6}$ s^{-1} (blue area in ***Figure 2b***) and approaches ~80% when $R_{bact} = 10^{-4}$ s^{-1} (purple area in ***Figure 2c***). Similarly, for organics with $K_H \sim 10^6$ M atm^{-1}, $R_{chemaq} = 10^{-9}$ s^{-1} and $R_{bact} = 10^{-6}$ s^{-1}, an increase in $R_{chemgas}$ from 10^{-6} s^{-1} (***Figure 2b***) to 10^{-5} s^{-1} (***Figure 2d***) and 10^{-4} s^{-1} (***Figure 2e***) decreases fr_{bact} from 73% to 23% and 3%. Based on these non-linear trends, one can hypothesize that (i) a change R_{bact} and/or $R_{chemgas}$ translates into a less than proportional change in fr_{bact}, and (ii) an increase of R_{bact} might translate into a larger change in fr_{bact} than an increase of $R_{chemgas}$ by the same factor. Therefore, fr_{bact} is more sensitive to a change in R_{bact} than in $R_{chemgas}$. Given that $R_{chemgas}$ only differs by about two orders of magnitude for most organics relevant in the atmospheric multiphase system (***Table 1***), we conclude that fr_{bact} may be largely independent of the gas phase chemical reactivity. Additional sensitivity studies (not shown) reveal that using combinations of R_{bact} and $R_{chemgas}$ other than those in ***Figure 2***, result in slightly different locations of the maximum of fr_{bact} but in similar shapes and widths of parameter spaces, for which fr_{bact} is maximum. Therefore, our conclusions on the sensitivities seem robust for wide parameters ranges and combinations.

3.1.2 fr_{bact} of CCN-derived compounds and comparison to water-soluble organic gases

For CCN-derived compounds, the analysis of fr_{bact} is limited to exploring the ranges of R_{bact} and R_{chemaq} (***Figure 1***). Similar to the findings based on ***Figure 2a, b and c*** for water-soluble organic gases, highest values of fr_{bact} are predicted for intermediate values of $10^{-10} \leq R_{bact}$ [s^{-1}] $\leq 10^{-7}$ and R_{chemaq} [s^{-1}] $\leq 10^{-10}$; for the highest biological activity ($R_{bact} = 10^{-4}$ s^{-1}), fr_{bact} is nearly zero (***Figure 3***). In order to understand the reasons for these trends, we explore in the following the variables determining fr_{bact} (Eq-7).
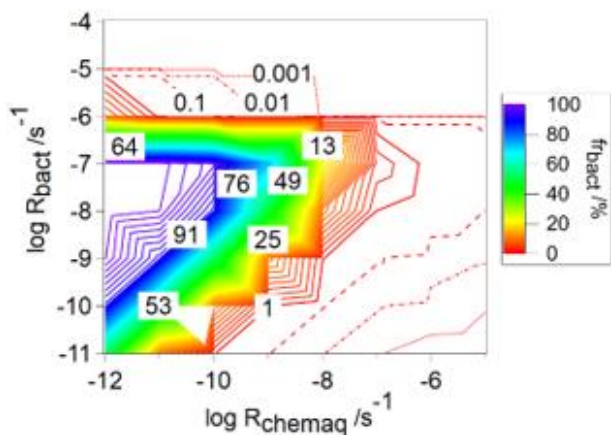
Figure 3: Relative contribution of bacteria to the total loss rate of CCN-derived organics (fr$_{bact}$, Eq-7) as a function of R$_{bact}$ [s^{-1}] and R$_{chemaq}$ [s^{-1}].

As shown in *Figure 1*, only one drop size class in the model contains bacteria; in all other droplets, the
275 bacterial activity is zero and only chemical processes occur. In *Figure 4a*, we show the evolution of the organic concentration of CCN-derived compounds in the bacteria-containing droplets ([Org]$_{bact}$) over 600s, R$_{chemaq}$ = 10^{-11} s^{-1} and R$_{chemgas}$ = 10^{-6} s^{-1}, i.e. for relatively low chemical reactivity in both phases. It is obvious that for the highest R$_{bact}$ (10^{-4} s^{-1}), the organics are immediately depleted whereas for lower biological activity (R$_{bact}$ = 10^{-6} s^{-1}), [Org]$_{bact}$ decreases more slowly or even stays constant (R$_{bact}$ = 10^{-8} s^{-1}). As for the highest
280 R$_{bact}$, the concentration approaches zero after ~10 seconds, R'$_{bact}$ (Eq-4) becomes negligible and fr$_{bact}$ approaches 0% (Eq-7, *Figure 4c*). In *Figure 4b*, we show the equivalent to *Figure 4a*, but for water-soluble organic gases and for three K$_H$ values (10^2, 10^5 and 10^9 M atm^{-1}). For the lowest R$_{bact}$ and all K$_H$ values, [Org]$_{bact}$ stays also nearly constant at the initial value as the organics are not efficiently consumed in any droplet. For the intermediate and highest R$_{bact}$ (10^{-6} and 10^{-4} s^{-1}) and K$_H$ = 10^9 M atm^{-1}, [Org]$_{bact}$ remains
285 higher than for the CCN-derived compounds and levels off at t ~300 seconds. For these two R$_{bact}$, [Org]$_{bact}$ significantly drops by several orders of magnitude. However, unlike for the CCN-derived compounds, fr$_{bact}$ does not drop to ~0% but levels off at ~70% for K$_H$ = 10^9 M atm^{-1} (*Figure 4d*). For these two R$_{bact}$ and K$_H$ = 10^5 M atm^{-1}, [Org]$_{bact}$ stays also nearly constant over the whole simulation time (600s) and is higher for lowest R$_{bact}$=10^{-6} s^{-1} (*Figure 4b*). However, fr$_{bact}$ is higher for the highest R$_{bact}$=10^{-4} s^{-1} (*Figure 4d*). *Figure*
290 *S3a* and *S3b* show the ratio of the organic concentrations in bacteria-containing and bacteria-free droplets of the same diameter (20 µm). For these conditions of low R$_{chemgas}$ and R$_{chemaq}$, the concentration ratio is near unity for both CCN-derived compounds and water-soluble organic gases (K$_H$ = 10^5 and 10^9 M atm^{-1}) when R$_{bact}$ = 10^{-8} s^{-1}. For higher R$_{bact}$ = 10^{-6} s^{-1} and K$_H$ = 10^5 and 10^9 M atm^{-1}, the concentration ratio for the water soluble organic gases is near unity and 10^{-3}, respectively and for the CCN-derived compounds it is much

295   lower (~10^{-6}). For $R_{bact} = 10^{-4}$ s^{-1}, this ratio is also higher for $K_H = 10^5$ M atm^{-1} than for $K_H = 10^9$ M atm^{-1} (~10^{-1} and 10^{-5} respectively) and $<<$ 10^{-11} for CCN-derived compounds. It can be summarized that (1) for water-soluble organic gases, the concentration in bacteria-containing droplets is higher for compounds with intermediate solubility ($K_H \sim 10^5$ M atm^{-1}) than for highly soluble ones ($K_H = 10^9$ M atm^{-1}) and (2) the concentration in bacteria-containing droplets is predicted to be always smaller for the CCN-derived

300   compounds than for the water-soluble organic gases with at least intermediate solubility.
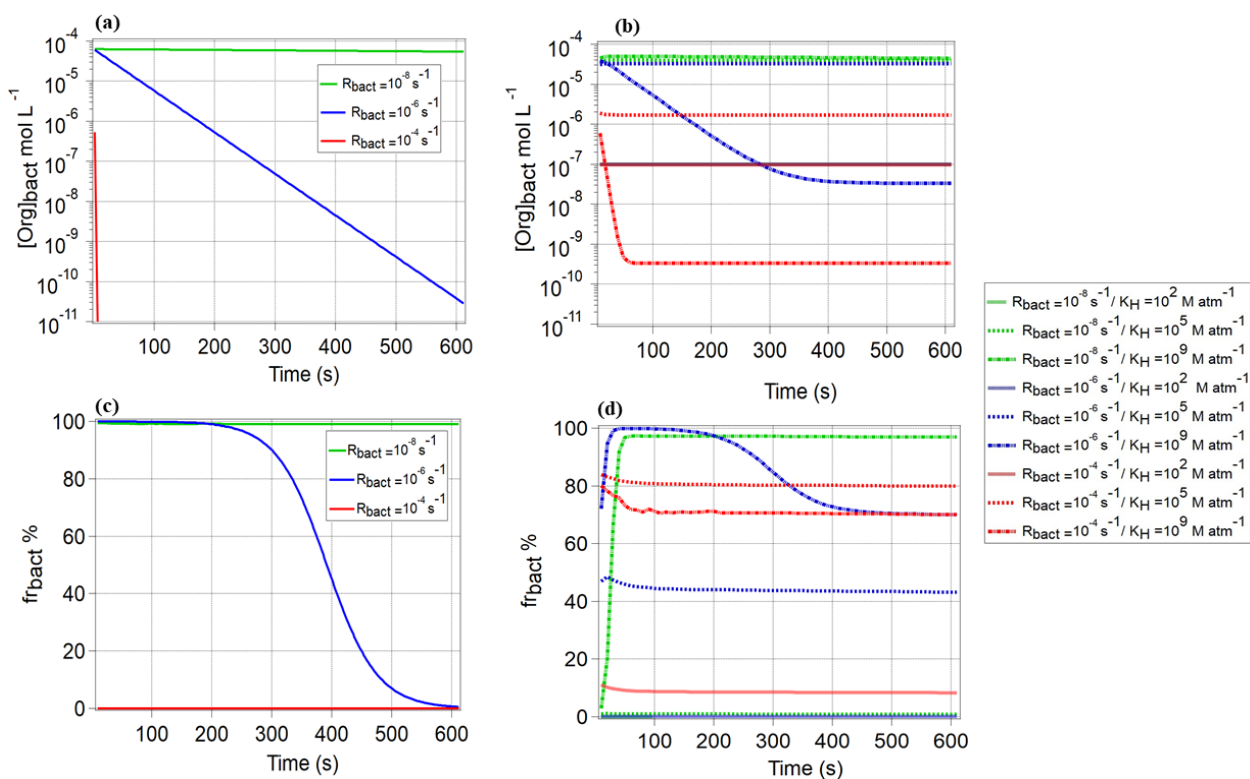
Figure 4. Comparison of the organic concentration in the bacteria-containing droplets [Org]$_{bact}$ [mol L^{-1}] for (a) CCN-derived compounds and (b) water-soluble organic gases ($K_H = 10^2$, 10^5 and 10^9 M atm^{-1}), and (c, d) the resulting fr$_{bact}$ for these compounds. Results are shown for $R_{bact} = 10^{-8}$, 10^{-6} and 10^{-4} s^{-1}, and $R_{chemgas} = 10^{-6}$ s^{-1}, $R_{chemaq} = 10^{-11}$ s^{-1}.

This difference between water-soluble organic gases and CCN-derived compounds can be explained by the schematic in *Figure 5*: The insets in the droplets schematically depict the temporal evolution of the organic concentrations as shown in *Figure 4*. The efficient consumption of organics by bacteria in the bacteria-containing droplets (I) leads to a significant decrease of the organic concentration in these droplets. For

305   water-soluble organic gases, this results in a strong deviation from thermodynamic equilibrium of the gas and aqueous phase concentrations, as defined by Henry's law (II). As a consequence, organics diffuse from the gas phase into the bacteria-containing droplets (III). As this diffusion leads to a decrease of the gas phase concentration, thermodynamic equilibrium between the gas phase and the bacteria-free droplets is not
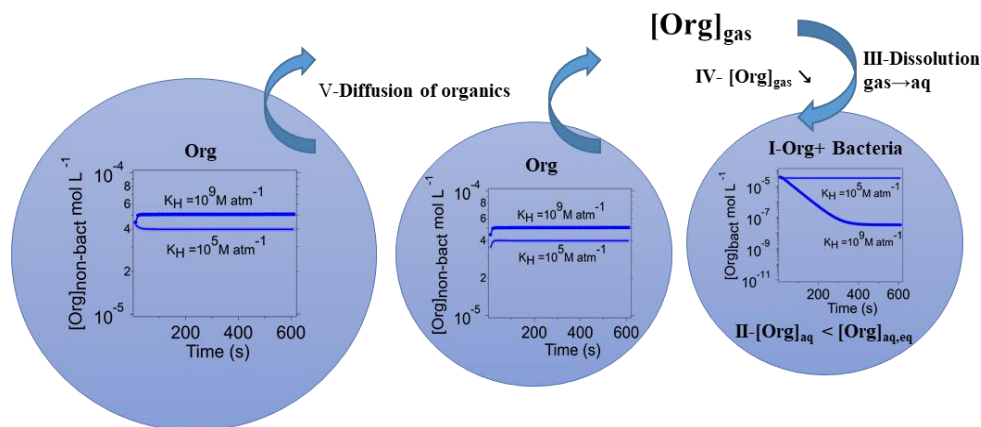
Figure 5. **:** Schematic of the partitioning of water-soluble organic gases between the bacteria-containing and bacteria-free droplets and the gas phase: The inset figures show the temporal evolution of the organic concentration in the bacteria-containing droplets ([Org]$_{bact}$) and bacteria free-droplets ([Org]$_{non-bact}$) for water-soluble organic gases with $K_H = 10^5$ M atm^{-1} and 10^9 M atm^{-1}.

fulfilled anymore (IV) resulting in a concentration gradient between these droplets and the gas phase.
Finally, organics from the bacteria-free droplets evaporate to replenish the gas phase concentration (V) and eventually the organic concentration in the bacteria-containing droplets. These coupled equilibria between the gas phase and droplets lead to a continuous replenishment of water-soluble organic gases in the bacteria-containing droplets. However, since all processes are associated with different time scales (evaporation, gas phase diffusion, transport through the gas/water interface, loss by chemical and biological processes in the aqueous phase (Schwartz, 1986), thermodynamic equilibrium is not instantaneously established. For organics with low K_H (~10^2 M atm^{-1}), the fraction of dissolved material is very small, therefore, organics are mostly consumed in the gas phase and only a small fraction partitions to the droplets. For intermediate K_H (~10^5 M atm^{-1}), the consumption of the organics in the bacteria-containing droplets is fast leading to large concentration gradients between the phases. Consequently, the evaporation and diffusion rates are high and thus the replenishment of the bacteria-containing droplets by the organics is most efficient. Extremely highly soluble organics (K_H ~ 10^9 M atm^{-1}) are nearly completely dissolved in the aqueous phase and thus, only a small fraction will be consumed by the bacteria leading to relatively smaller concentration gradients between gas and bacteria-containing droplets (Process I and *Figure 4b*) and therefore to less efficient replenishment and longer time scales to establish thermodynamic equilibrium. Thus for such organics, the organic consumption by bacteria is relatively less efficient. For CCN-derived compounds, only Process I occurs as there is no coupling to the gas phase and thus, only the amount of organics that is initially dissolved in the bacteria-containing droplets can be consumed.

3.2   Total loss of the organic compound (L_t) and sinks of organics by bacteria (L_{bact})

3.2.1 L_t for water-soluble organic gases

330   While the analysis of fr_{bact} in **Section 3.1** quantifies the relative importance of the biological and chemical processes for the organic loss, we explore in the following the absolute loss of these processes (L_t, Eq-10). Unlike the sum of fr_{bact}, fr_{chemaq}, and $fr_{chemgas}$ that always yields 100%, the ranges of L_t that will be discussed in the following are rather small, i.e. $10^{-4} \leq L_t [\%] \leq 12$, given that we only simulate approximately one cloud cycle (600s). **Figure 6** shows L_t for the same parameters ($R_{chemgas}$, R_{bact}) as in **Figure 2**. For all combinations

335   of R_{bact} and $R_{chemgas}$, the highest values of L_t are predicted for organics with highest K_H and R_{chemaq}. Generally, all panels show the highest values for L_t for the highest R_{chemaq} but in all panels there is a small maximum, for low to intermediate K_H and nearly independent of R_{chemaq}. This feature becomes more prominent with increasing $R_{chemgas}$ (10^{-6} s^{-1}, 10^{-5} s^{-1}, 10^{-4} s^{-1}, **Figure 6c-e**), with the overall highest L_t (~12%) for the highest $R_{chemgas}$ and lowest K_H. Comparing **Figure 6a, b, and c**, for which the model conditions only differ in R_{bact},

340   a small increase in L_t from 1.2% to 1.6% at intermediate K_H values can be seen. We focus on these trends in **Section 3.2.2** where L_{bact}, i.e. the contribution of the bacterial process to L_t, will be explored. Comparing the shapes of the three panels, shows that L_t is additive as with increasing R_{bact}, L_t reaches a maximum (1.6%) at $K_H \sim 10^4$ M atm^{-1} and $R_{chemaq} \sim 10^{-5}$ s^{-1} (**Figure 6c**). Similar to our findings for fr_{bact} (**Section 3.1.1.**), we also see in the trends of L_t that a change of several orders of magnitude in R_{bact} or $R_{chemgas}$ translates into a

345   smaller change in L_t. Thus, one can conclude that L_t has a similarly low sensitivity to the various parameters as fr_{bact}.
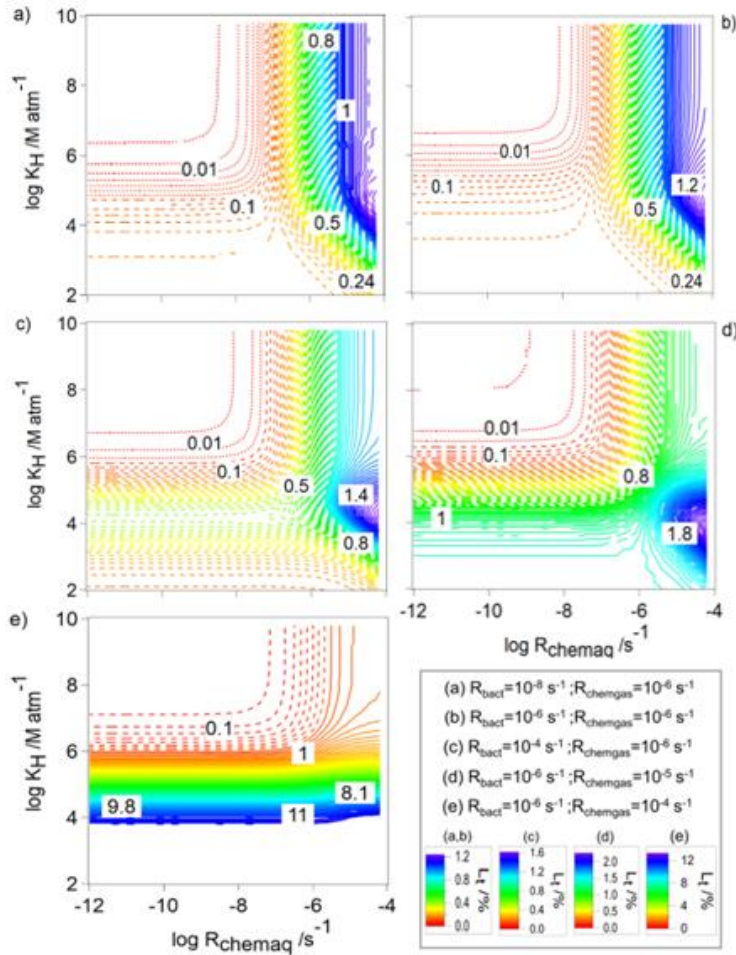
Figure 6: The total loss of water-soluble organic gases (L_t, Eq-10) as a function of R_{chemaq} and K_H. All figure panels have the same scales on the ordinates and abscissas, respectively. The simulations were performed for constant values of R_{bact} and $R_{chemgas}$; their values are indicated in the box at the bottom right.

3.2.2 L_{bact} for water-soluble organic gases

To understand the contribution of bacteria (L_{bact}) in the total consumption of the organics (L_t), we explore L_{bact} for the same values of R_{bact} and $R_{chemgas}$ as in *Figures 2* and *6* (*Figure 7*). As suggested in the comparison of *Figures 6a-c*, the contribution of the organic loss by bacteria increases with increasing R_{bact} (*Figure 7a-c*), i.e. L_{bact} increases from 0.025% to 0.45%.

For all conditions, there is a contribution of $L_{bact} \sim 0.025\%$ for the lowest R_{chemaq} and highest K_H, i.e. when chemical activity in the aqueous phase is lowest and solubility is highest. However, when $R_{bact} \geq 10^{-6}$ s^{-1}, the maximum value of L_{bact} is predicted for a narrow range of $\sim 10^4 \leq K_H$ [M atm^{-1}] $\leq 10^6$, nearly independent of R_{chemaq}. The highest value of L_{bact} (0.4%) is observed for highest R_{bact} ($R_{bact} = 10^{-4}$ s^{-1}; *Figure 7c*). This

corresponds to nearly a quarter of the total loss ($L_t \leq 1.4\%$, **Figure 6c**). To further explore why L_{bact} has a maximum for this intermediate values of K_H, we compare L_{bact} for $K_H = 10^2$ M atm^{-1}, 10^5 M atm^{-1} and 10^9 M atm^{-1} for $R_{bact} = 10^{-6}$ s^{-1}, $R_{chemgas} = 10^{-6}$ s^{-1} and $R_{chemaq} = 10^{-11}$ s^{-1}, i.e. for the same conditions as the examples

360   in **Figure 4b** and **d**. When K_H is low (10^2 M atm^{-1}), a very small fraction (0.16%) of the organics is dissolved and, thus, L_{bact} is lowest. For $K_H = 10^9$ M atm^{-1} (**Figure 4b**, blue line), $[Org]_{aq}$ is low because - as mentioned before - it is consumed quickly and the transport from the gas phase is not fast enough resulting in a low L_{bact}. For $K_H \sim 10^5$ M atm^{-1} (**Figure 4b**, blue line), $[Org]_{aq}$ is relatively high because the thermodynamic equilibrium can be more quickly established and, thus, L_{bact} is high.

365   For each set of conditions, i.e. in the various panels of **Figure 7**, the maximum value L_{bact} is independent of R_{chemaq} and does not greatly vary for the same R_{bact} ($L_{bact,max} \sim 0.05\%$) (**Figure 7b, d, e**). This is different than the trends of fr_{bact} (**Figure 2**) that show a decrease with increasing R_{chemaq}. By definition (Eq-7), fr_{bact} and fr_{chemaq} are coupled and thus an increase in one value causes a decrease in the other. Contrary, L_{bact} is independent of the chemical contributions as it describes the absolute consumption rate related to the initial

370   organic concentration. Comparing the trends in **Figures 2 and 7**, it is evident that the maximum of L_{bact} (intermediate K_H, independent of R_{chemaq}) does not coincide with the parameter ranges for which fr_{bact} is maximum (highest K_H, lowest R_{chemaq}). This finding highlights that previous estimates on the importance of biodegradation that were solely based on comparing rates (e.g., Jaber et al., 2020) are misleading. In these studies, it was concluded that biodegradation for highly soluble compounds is likely most important.
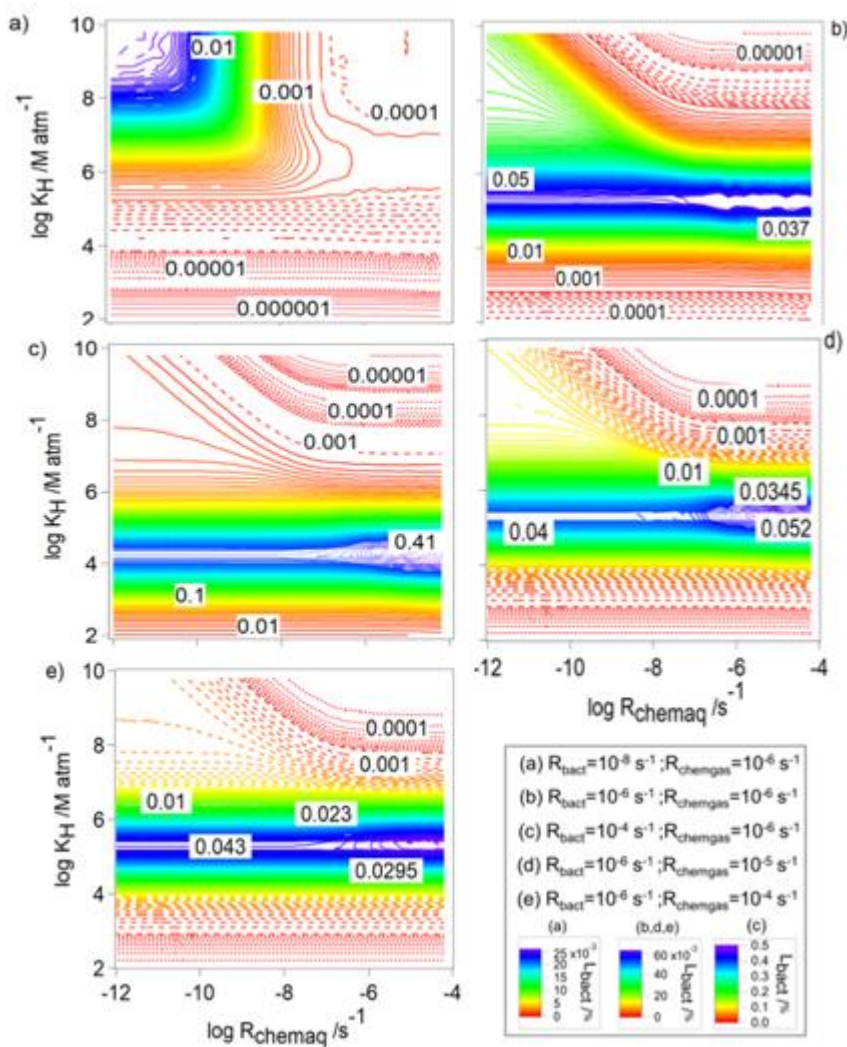
Figure 7. The loss of water-soluble organic gases by bacteria (L_{bact}, Eq-11) as a function of R_{chemaq} and K_H. All figure panels have the same scales on the ordinates and abscissas, respectively. The simulations were performed for constant values of R_{bact} and $R_{chemgas}$; their values are indicated in the box at the bottom right.

375

3.2.3 L_t and L_{bact} for CCN-derived compounds

For CCN-derived compounds, the analysis of trends in L_t is simpler as it is the sum of L_{bact} and L_{chemaq} only. L_t increases with increasing R_{chemaq}, nearly independently of R_{bact} up to a maximum value of ~1.1% (*Figure 8a*). Comparison of L_t to L_{bact} (*Figure 8b*) shows that the consumption by bacteria is smaller by several orders of magnitude ($L_{bact,max} = 0.005\%$) and thus it is not a major contribution to the total loss. *Figures 3 and 8b* exhibit similar shapes, i.e. after 600 seconds simulation time, the highest relative and absolute contributions are predicted for CCN-derived compounds with intermediate bacterial and low aqueous phase

chemical activity. The trend in *Figure 8b* can be also explained by the findings in *Figure 4*: After 600 seconds, the CCN-derived compounds in the bacteria-containing droplets are completely depleted for high R_{bact} and thus both fr_{bact} and L_{bact} approach zero. Since there is no exchange with the gas phase or other replenishment of CCN-derived compounds into bacteria-containing droplets, $L_{bact,maximum}$ of these compounds can be estimated: If one assumes in a first approximation that the mass fraction of CCN-derived compounds in the initial CCN population scales with the liquid water content associated with the resulting droplets, one can conclude that at most 0.0065% (=LWC(bacteria-containing droplets/total LWC) can be consumed.
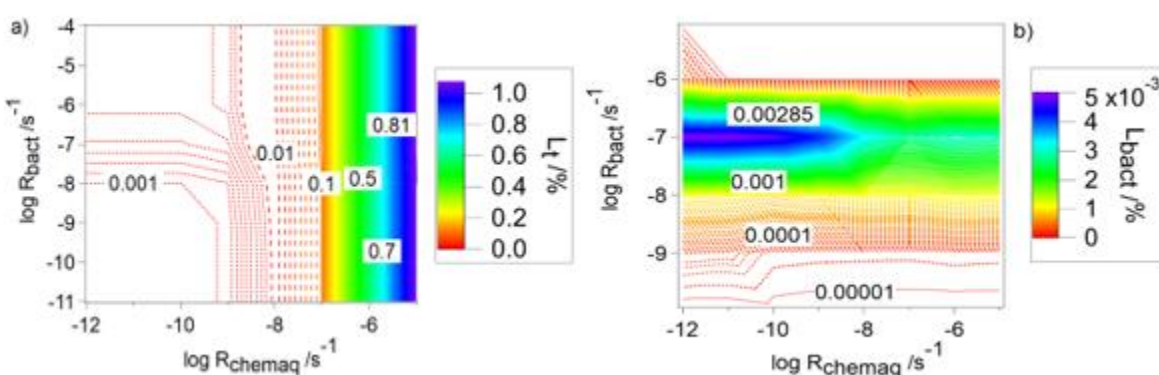
Figure 8. Predicted loss of CCN-derived species as a function of R_{chemaq} and R_{bact}, a) total loss (L_t), b) loss by biodegradation (L_{bact}).

3.3   Comparison of our model approach to simplified assumptions

3.3.1   Simplified model approaches

The results in *Figures 4,* demonstrate that the coupled equilibria between the gas phase and the droplets with and without bacteria need to be considered, in order to correctly predict the organic sink strength by bacterial processes in the multiphase system. Previous estimates of the role of biodegradation in the multiphase system have been performed assuming simplified assumptions: (i) Bulk model: Biodegradation and chemical rates were compared in a bulk aqueous phase (Vaïtilingom et al., 2013b) or in a population of droplets with identical composition (Jaber et al., 2020). However, since the bacteria cell concentration (~ 0.01 cells cm^{-3}) in clouds is much smaller than the droplet number concentration (= 263 droplets cm^{-3}, in our model), this results in a ratio of $\sim 4.10^{-5}$ bacteria cells per droplet. (ii) Low-LWC model: multiphase system is considered with only droplets that contain an intact bacteria cell resulting in a liquid water content of $\sim 10^{-11}$ vol/vol, similar to (Fankhauser et al., 2019). In *Figure 9*, we schematically contrast these approaches. While it is clear, that none of the two approaches reflect the conditions as encountered in real

405 clouds, we will analyze in the following the extent to which these simplified model approaches lead to similar results as predicted in our detailed model discussed so far (***Figure 1***).

3.3.2 Comparison of fr_{bact}, L_t and L_{bact} using simplified model approaches

For water-soluble organic gases, we compare fr_{bact} and L_{bact} for the three model approaches for the full range of K_H values, $R_{bact} = 10^{-6}$ s^{-1}, $R_{chemaq} = 10^{-7}$ s^{-1} and $R_{chemgas} = 10^{-6}$ s^{-1} (***Figure 9 a, b***). For $10^2 \leq K_H$ [M atm^{-1}] $\leq$
410 10^4, only a small difference in fr_{bact} and L_{bact} is predicted for a given R_{bact} because of the low organic fraction in the aqueous phase. For all K_H values, fr_{bact} is the highest for the low LWC model approach, because it only considers bacteria-containing droplets and, thus, neglects the aqueous phase chemistry in a majority of droplets; therefore, fr_{chemaq} is significantly underestimated. Consequently, the competition between biodegradation and chemical degradation takes place only in the bacteria-containing droplets and fr_{bact} is the
415 highest.

For $10^5 \leq K_H$ [M atm^{-1}] $\leq 10^7$, L_{bact} based on the bulk and low LWC models are higher than for the detailed model. For example, for $K_H = 10^6$ M atm^{-1}, L_{bact} in the low-LWC model is 4.3 and 12.7 higher than in the bulk and our detailed models. For the highest K_H ($10^7 \leq K_H$ [M atm^{-1}] $\leq 10^9$), the comparison of L_{bact} for $R_{bact} = 10^{-6}$ s^{-1} shows that both simplified model approaches overestimate L_{bact} by up to several orders of
420 magnitude (***Figure 9b***) for $K_H = 10^8$ M atm^{-1} ($L_{bact,lowLWC} = 5.8 \times 10^{-1}$; $L_{bact,bulk} = 1.07 \times 10^{-1}$; $L_{bact,detailed} = 6.12 \times 10^{-4}$). For organics with intermediate or low solubility, the differences between the three models are smaller. Given that we identified biodegradation to be most important for organics with intermediate solubility (***Section 3.2.2***), we compare fr_{bact} and L_{bact} for $K_H = 10^5$ M atm^{-1}, $R_{chemgas} = 10^{-6}$ s^{-1}, $R_{chemaq} = 10^{-7}$ s^{-1} as a function of R_{bact} (***Figure 9 c, d***). Similar to the results from the detailed model (***Section 3.1.2***), the low
425 LWC approach leads to $fr_{bact} < 100\%$ at t = 600s because organics are efficiently consumed in the bacteria-containing droplets. However, for the bulk model, $fr_{bact} \sim 100\%$ for the highest R_{bact}, even after 600s, because bacterial processes take place in all droplets with a reduced efficiency as compared to the processes in the single droplet in the detailed model. Consequently, the concentration of organics in all droplets remains relatively high for extended time scales, even for the highest R_{bact}. ***Figure 9d*** shows the dependence of L_{bact}
430 between the three models on R_{bact}: for $R_{bact} \leq 10^{-6}$ s^{-1}, L_{bact} is similar for the detailed and the bulk models (~5 $\times 10^{-4}$ %) whereas it is twice as high for the low LWC model (~1×10^{-3} %). However, for the highest R_{bact} (10^{-4} s^{-1}), the highest L_{bact} is predicted by the bulk approach (~5%) which is more than two orders of magnitude higher than predicted from the detailed model (~0.2 %). The similarity of L_{bact} between the detailed and the bulk models for $R_{bact} = 10^{-6}$ s^{-1} is due to the efficient replenishment of organics with
435 intermediate K_H (***Figure 5***), i.e. the amounts of organics available to bacteria are similar. However, for the highest R_{bact}, L_{bact} is much higher for the bulk model because the consumption of the organics occurs without any kinetic limitations of the various transport processes that are only presented by the detailed model.
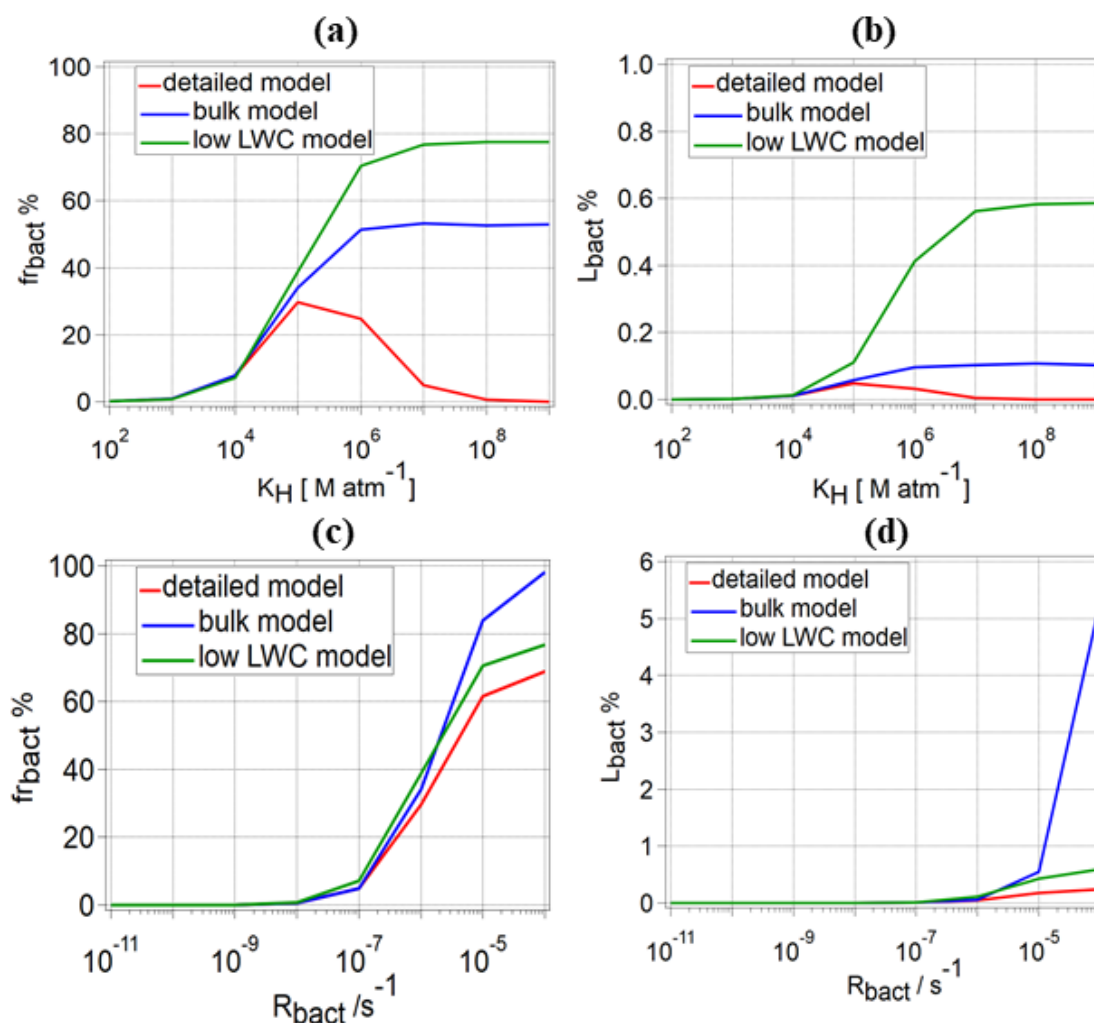
Figure 9: Comparison of (a) fr_{bact}, (b) L_{bact} for water-soluble organic gases for three the different model approaches: detailed model (red line), bulk approach (blue line) and low LWC model (green line) for different K_H, $R_{chemaq}=10^{-7}\,s^{-1}$, $R_{bact.}=10^{-6}\,s^{-1}$ and $R_{chemgas} = 10^{-6}\,s^{-1}$; (c) fr_{bact} and (d) L_{bact} for water-soluble organic gases for the same approaches for different R_{bact} , one $K_H= 10^{5}\,M\,atm^{-1}$, two R_{chemaq}: $10^{-7}\,s^{-1}$, $R_{chemgas}=10^{-6}\,s^{-1}$

For the CCN-derived compounds, we compare fr_{bact} and L_{bact} for different R_{bact} and two R_{chemaq} (10^{-11} and $10^{-7}\,s^{-1}$) (***Figure S4 a, b***). For $R_{bact}= 10^{-8}\,s^{-1}$ and $R_{chemaq} = 10^{-11}\,s^{-1}$, fr_{bact} is about 99% for all three approaches which is not the case for highest R_{chemaq} ($10^{-7}\,s^{-1}$) (***Figure S4a***). However, for $R_{bact} = 10^{-4}\,s^{-1}$, fr_{bact} is ~0% (at t = 600s) in the detailed model for both R_{chemaq} for the reasons explained in ***Section 3.1.2*** whereas fr_{bact} ~ 99% for the bulk model because of continuous bacteria activity in all droplets. Moreover, fr_{bact} and L_{bact} are always 100% for the low-LWC model. The role of aqueous phase chemistry in the multiphase system is predicted to be negligible by the low-LWC approach as it is equally reduced as the LWC, leading to the dominance of the bacterial processes. If we compare L_{bact} for the bulk (blue line in ***Figure S4b***) and the

detailed models (red line), one finds an increasing discrepancy between the model results: For the lowest R_{bact} considered here (10^{-8} s^{-1}) and the two R_{chemaq}: 10^{-11} s^{-1} and 10^{-7} s^{-1} respectively, L_{bact} for the bulk model is predicted to be $\sim$ 9.3 and 11.6 times higher than for the detailed model. For $R_{bact} = 10^{-6}$ s^{-1} and the two R_{chemaq}, this factor increases to 2.5×10^4 and 1.3×10^6. For the highest $R_{bact} = 10^{-4}$ s^{-1}, L_{bact} between the bulk and our detailed model after 600s of simulation cannot be reasonably compared as in the detailed model after < 100 seconds, the CCN-derived compounds in the bacteria-containing droplets are completely depleted for high R_{bact} and, thus, no further consumption occurs ($L_{bact} \sim$ 0%) (*Section 3.2.3*). In the bulk model, the organic consumption by bacteria is predicted to occur continuously as the bacteria could, in theory, consume all organics on 'infinite' time scales.

Our model comparison shows that for water-soluble organic gases and CCN-derived compounds, both the bulk and low-LWC models overestimate the importance of biodegradation, i.e. both fr$_{bact}$ and L_{bact}. The biases are highest in the bulk approach for high R_{bact} and high K_H. Also, the comparison shows that the bulk approach leads to wrong conclusions in terms of the importance of biodegradation as a function of the solubility of organics. Our model analysis emphasizes that a detailed model is needed in order to correctly represent the partitioning of water-soluble organic gases between the gas phase and the droplets with and without bacteria.

4. Atmospheric implications: How important is biodegradation for organic compounds identified in cloud water?

4.1 L$_{bact}$ of organic cloud water constituents

Based on our model sensitivity studies discussed in the previous sections and the literature data for cloud water organics summarized in *Tables 1* and *2*, we assess the importance of biodegradation of these compounds. The contour plot representations in *Figure 10* are the same as in Figures *7 a-c* (water soluble organic gases) and *Figure 8b* (CCN-derived compounds), respectively. The added symbols correspond to L_{bact} of the compounds in *Table 1* for a single R_{bact} in each figure panel. Given that $R_{chemgas}$ only differs by about two orders of magnitude for the organics in *Table 1*, we present the results with $R_{chemgas} = 10^{-6}$ s^{-1}. The reasoning of the assumed single R_{bact} is further discussed in *Section 4.2*.

For the carboxylic acids, two values are shown, i.e. $K_{H(eff)}$ and R_{chemaq} at pH = 3 and 6 (*Table 3*). R_{chemaq} at the two pH values are calculated based on the rate constants k_{chemaq} as a function of the proportion of the acidic and anionic forms depending on pH and pK_a and the rate constants of the OH reactions for the acid and anion. Similarly, rate constants for other (e.g. NO$_3$) reactions could be derived using data summarized in *Table 1*.

As discussed in **Section 2.2.2** and by Vaïtilingom et al. (2013), the bacterial activity does not show any systematic difference in this pH range; therefore, we only show one R_{bact} value for each acid. For the lowest R_{bact} (10^{-8} s^{-1}), the physicochemical properties ($K_{H(eff)}$, R_{chemaq}) of the water-soluble organic gases (acetic acid/acetate, formic acid/formate, formaldehyde, catechol, phenol and methanol) are in the range where L_{bact} has its minimum values $\sim 10^{-6} \leq L_{bact}$ [%] $\leq 10^{-3}$ (**Figure 10a**).
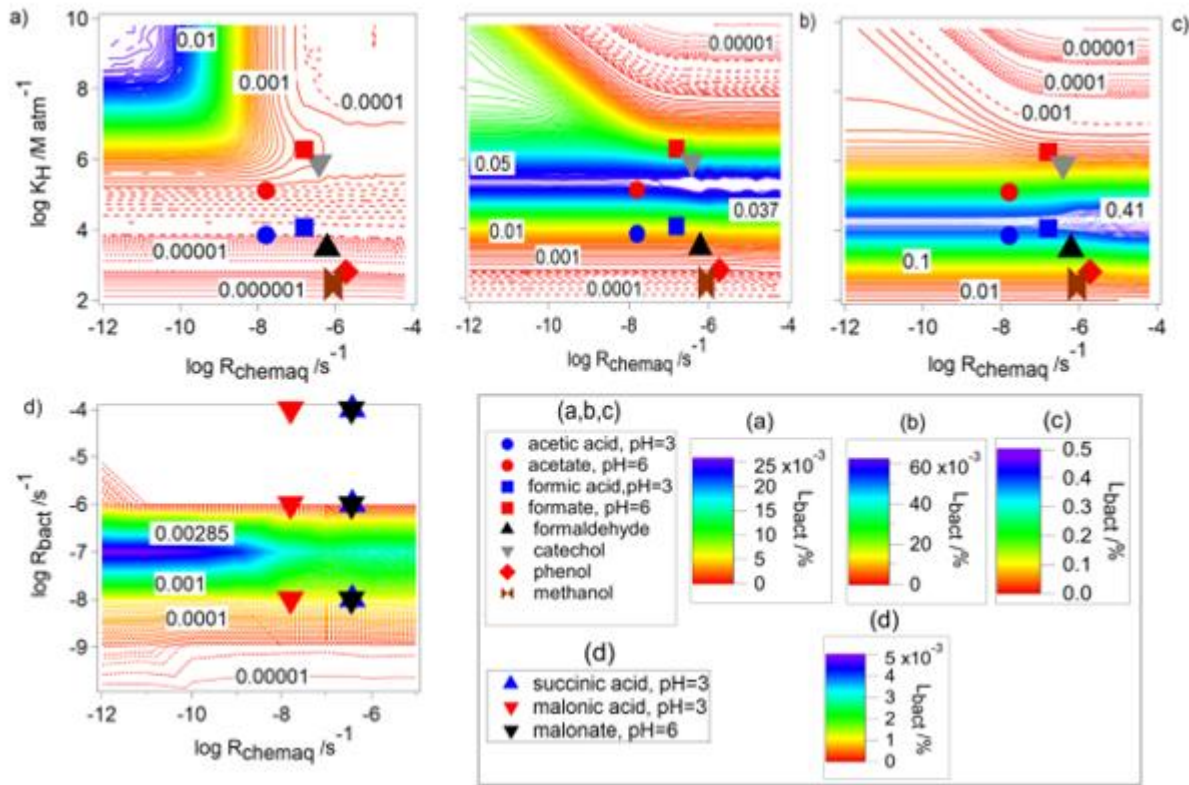
Figure 10: a) – c) L_{bact} for water-soluble organic gases. The contour plots are identical to Figure 7a-c. Symbols show combinations of R_{chemaq} and K_H for specific compounds (Table 1). For all simulations $R_{chemgas} = 10^{-6}$ s^{-1}; a) $R_{bact} = 10^{-8}$ s^{-1} b) $R_{bact} = 10^{-6}$ s^{-1} c) $R_{bact} = 10^{-4}$ s^{-1}

d) L_{bact} for CCN-derived organics (Table 1). The contour plot is identical to Figure 8b). Note that R_{chemaq} and R_{bact} for succinate (pH = 6) are nearly identical to the values for succinic acid (pH = 3) and were therefore omitted from the figure.

For higher R_{bact} (10^{-6} s^{-1}, **Figure 10b**), which implies higher cell concentration in the cloud, highly soluble compounds, such as acetate and catechol, are in the range where L_{bact} shows a maximum ($\sim 0.04 \leq L_{bact}$ [%] ≤ 0.06) and less soluble compounds such as formic acid, formate and formaldehyde ($10^4 < K_{H(eff)}$ [M atm^{-1}] $< 10^6$) are in the area where $\sim 0.02 \leq L_{bact}$ [%] ≤ 0.04. Less soluble compounds ($K_{H(eff)} < 10^3$ M atm^{-1}), such as acetic acid, phenol and methanol are in the area of much lower L_{bact} ($\sim 10^{-5} \leq L_{bact}$ [%] $\leq 10^{-3}$). As discussed in **Section 3.2**, the maximum value of L_{bact} increases with higher R_{bact} and is predicted for compounds with moderate $K_{H(eff)}$ (**Figure 5**). Therefore, at the highest assumed R_{bact} (10^{-}

490   ^{4} s^{-1}), the less soluble compounds formic acid, formaldehyde and acetic acid, are in the range where L_{bact} has

its maximum values ($0.3 < L_{bact}$ [%] < 0.4; ***Figure 10c***).

Figure 10d repeats the full parameter ranges of R_{bact} and R_{chemaq}. We discuss L_{bact} for the CCN-derived

compounds (malonic acid, malonate, succinic acid, succinate) for the same R_{bact} as in ***Figure 10 a-c***:The

maximum consumption of CCN-derived compounds by bacteria corresponds to the fraction of the organics

495   present in bacteria-containing droplets (~0.0065% in our simulations). Therefore, the predicted L_{bact} [%]

are very similar for all compounds considered here (malonate/malonic acid and succinate/succinic acid) and

does not differ, independently of R_{bact}.

4.2   Dependence of L_{bact} on bacteria cell concentration in cloud water

According to **Eq-3**, R_{bact} is the product of the biodegradation rate constant k_{bact} [L Cell^{-1} s^{-1}] (***Table2***) and

500   the cell concentration C_{cell} [Cell L^{-1}]. Based on the three R_{bact} values and the k_{bact} data for the various organics,

we calculate $C_{cell,theoretical}$ that would be needed to reach these R_{bact} :

$$C_{cell,theoretical} \; [Cell \; L^{-1}] = \frac{R_{bact} \; [s^{-1}]}{k_{bact} \; [L \; Cell^{-1} \; s^{-1}]} \qquad\qquad \text{Eq-14}$$

The resulting $C_{cell,theoretical}$, [Cell L^{-1}] are listed in ***Table 3***, together with k_{bact} [L Cell^{-1} s^{-1}]. Among the water-

soluble organic gases, $C_{cell,theoretical}$ is predicted to be ~$10^2 \leq C_{cell,theoretical}$ [Cell L^{-1}] $\leq 10^7$ for acetic acid, formic

505   acid and phenol while it is much higher (~$10^7 \leq C_{cell,theoretical}$ [Cell L^{-1}] $\leq 10^{15}$) for catechol, formaldehyde

and methanol that have much lower k_{bact} than the former compounds. Typical bacteria cell concentration in

cloud water are in the range of 10^6 - 10^8 Cell L^{-1} (Amato et al., 2007c). Comparing this range to $C_{cell,theoretical}$

reveals that for several compounds $C_{cell,theoretical}$ falls into a realistic range (grey shaded cells in ***Table 3***): for

ambient cell concentrations in cloud water, malonic acid/malonate, succinic acid/succinate, acetic

510   acid/acetate, formic acid/formate, cathecol and phenol might fall into a range where the maximum

consumption of organics by biodegradation can be expected, while for formaldehyde and methanol

$C_{cell,theoretical}$ is unrealistic ($\geq 10^9$ cells L^{-1}) based on the available studies of bacteria cell concentrations in

cloud water.

Table 3. k_{bact} [L Cell^{-1} s^{-1}] calculated from literature data, theoretical C_{cell} [Cell L^{-1}] based on Eq-14 and the
515   ratio L_{bact}/L_t for three R_{bact} (10^{-8} s^{-1}, 10^{-6} s^{-1} and 10^{-4} s^{-1}) for water-soluble organic gases and CCN-derived compounds. Grey-shaded cells show bacteria concentrations, realistic for cloud water.

Organic compound	k_{bact} [L Cell^{-1} s^{-1}]	$C_{cell,theoretical}$ [Cell L^{-1}] based on Eq-14			$L_{bact,max}$ [%]		
		R_{bact}			R_{bact}		
		10^{-8} s^{-1}	10^{-6} s^{-1}	10^{-4} s^{-1}	10^{-8} s^{-1}	10^{-6} s^{-1}	10^{-4} s^{-1}
CCN-derived compounds							
Malonic acid Malonate	9.0×10^{-13}	3.3×10^4	3.3×10^6	1.1×10^8	$\leq 0.0065\%$ (= LWC$_{bact}$ / / LWC$_{total}$		

					L_{bact}/L_t	L_{bact}/L_t	L_{bact}/L_t
Succinic acid, Succinate	3.0×10^{-13}	3.3×10^{4}	3.3×10^{6}	3.3×10^{8}			
water soluble organic gases							
Acetic acid Acetate	4.7×10^{-11}	2.1×10^{2} 7.1×10^{3}	2.1×10^{4} 7.1×10^{5}	2.1×10^{6}	5.8×10^{-4} 8.0×10^{-2}	5.8×10^{-2} 3.3×10^{-1}	7.0×10^{-1} 6.7×10^{-1}
Formic acid Formate	1.4×10^{-12}	7.1×10^{3} 1.4×10^{9}	7.1×10^{5} 1.4×10^{11}	7.1×10^{7}	6.2×10^{-4} 1.2×10^{-3}	7.4×10^{-2} 2.6×10^{-2}	6.5×10^{-1} 3.4×10^{-2}
Formaldehyde	7.0×10^{-18}	3.6×10^{6}	3.6×10^{8}	1.4×10^{13}	8.4×10^{-4}	7.4×10^{-2}	6.5×10^{-1}
Catechol	2.7×10^{-15}	3.0×10^{2}	3.0×10^{4}	3.6×10^{10}	3.5×10^{-3}	1.2×10^{-1}	2.0×10^{-1}
Phenol	3.3×10^{-11}	1.2×10^{11}	1.2×10^{13}	3.0×10^{6}	5.4×10^{-5}	5.4×10^{-3}	3.2×10^{-1}
Methanol	8.1×10^{-20}	1.2×10^{11}	1.2×10^{13}	1.2×10^{15}	2.3×10^{-5}	2.3×10^{-3}	2.4×10^{-1}

4.3   For which organics is biodegradation an efficient sink in the atmosphere?

The maximum value of L_{bact} is ~0.7% in all our simulations but one should keep in mind that also the predicted L_t is not higher than a few percent (***Figure 6 a-c***) as we restrict our simulations to the time scale of approximate one cloud cycle. However, in a relative sense, our results allow us to compare the importance of biodegradation to chemical loss for the compounds shown in ***Figure 10***. To quantify the contribution of bacteria to the total consumption (L_t) we list the ratio L_{bact}/L_t in ***Table 3***. Our results clearly show that biodegradation might add significantly to the loss of formic acid/formate ($L_{bact}/L_t = 0.65$) and acetic acid/acetate ($L_{bact}/L_t = 0.70$) at cell concentrations of ~$7\cdot10^7$ and $2\cdot10^6$ Cells L^{-1}, respectively. These acids contribute on average ~68% to the total dissolved carbon in cloud and fog water (Herckes et al., 2013). Their removal by dry and wet deposition are considered the major loss processes in the atmosphere (Khare et al., 1999). However, several studies also suggested that the oxidation for formic acid/formate in cloud water may be a net sink (Jacob, 1986). Measurements during different seasons in the Amazon showed that indeed formic and acetic acids have stronger sinks during the wet season (Herlihy et al., 1987). While wet deposition was described to contribute to a large extent to the observed removal, chemical and possibly bacterial processes were suggested to act as additional sinks. While the latter was regarded as being inefficient due to long incubation time as observed in lab experiments, more recent experiments suggest that such incubation times are likely not occurring in the atmosphere where bacteria cells are continuously exposed to water and substrates (Amato et al., 2007a; Vaïtilingom et al., 2010b, 2013a). We conclude that biodegradation of these major cloud water organics may be a significant sink under ambient conditions, possibly even comparable to the loss by chemical reactions. While phenol is not a major contributor to the WSOC content in cloud water (5-95 nM) (Jaber et al., 2020) as compared to 10 µM (Ervens et al., 2003b; Löflund et al., 2002; Sun et al., 2016) for formic and acetic acids respectively, its degradation processes in

540   the atmosphere might be of interest due to its toxic properties. Overall, our results are in agreement with previous findings that neither chemical processes nor biodegradation are major WSOC losses as compared to deposition (Ervens and Amato, 2020; Fankhauser et al., 2019). However, in order to comprehensively describe the loss processes and time scales of organic degradation and residence time scales in the atmosphere, both chemical and biological processes should be considered. Hence, we suggest that biological

545   processes of organics with properties similar to those of formic and acetic acids and phenol ($\sim 10^3 < K_{H(eff)}$ [M atm^{-1}] $< \sim 10^6$, $k_{bact} = 10^{-11}$ s^{-1}) should be included in atmospheric multiphase models.

The importance of biodegradation of CCN-derived compounds is limited by the number fraction of cloud droplets that contain bacteria. Malonate/malonic acid and succinate/succinic acid contribute on average to < 5% to the total organic aerosol mass in ambient particles, e.g. (Fu et al., 2013; Kawamura and Ikushima,

550   1993). Their loss by chemical and biological processes will neither affect the total carbon budget to a large extent nor the budget of the individual compounds. These conclusions can be generalized for other CCN-derived aerosol constituents, for which biodegradation has been suggested to occur in the atmosphere. Our assumption of static cloud droplets in the box model is certainly a simplified representation of cloud microphysics. Droplets might experience collision/coalescence in clouds leading to mixing of the cloud

555   water constituents in the resulting larger droplets. However, such processes are unlikely to add significantly to the loss of CCN-derived compounds by bacteria due to (i) the number small fraction of bacteria-containing droplets (0.001 – 0.0001) and (ii) the limited atmospheric residence time of large droplets which are efficiently removed by precipitation as a function of drop size (Beard and Ochs, 1984).

5.   Summary and Conclusions

560   Our model sensitivity study is the first comprehensive analysis of the importance of biodegradation of organics by bacteria in the atmospheric multiphase system in comparison to chemical loss for wide ranges of chemical and biodegradation kinetic data. We use a box model with drop-size-resolved aqueous phase chemistry and additional biological processes that only occur in a small number of cloud droplets, in agreement with ambient ratios of cell and droplet concentrations. We neglect the fact that bacteria cells may

565   form agglomerates in the atmosphere and consequently, there might be more than one cell per droplet. This effect could be included in our model by multiplying the biological activity in the respective droplets with the number of cells.

We compare the predicted loss rates of chemical processes in both phases to those of biological processes in the aqueous phase only. In addition to presenting the relative loss rates (fr_{bact}, fr_{chem}) as in previous studies

570   (Jaber et al., 2020; Vaïtilingom et al., 2010a), we discuss the relative amounts of organics (L_t) consumed by chemical (L_{chem}) and biological processes (L_{bact}). We find that the relative loss rate of organics by biological processes (fr_{bact}) is generally higher for water-soluble organic gases than for CCN-derived compounds.

However, the total loss of the organics (L_t) is predicted not to reach any value higher than ~12% because our simulations were restricted to a period of 600s (~ drop lifetime within one cloud cycle); it would be higher if the total particle processing time during multiple cloud cycles in the atmosphere were considered. The contribution of bacteria (L_{bact}) to the total loss is predicted to be highest for water-soluble organic gases with intermediate solubility ($\sim 10^4 \leq K_H$ [M atm^{-1}] $\leq \sim 10^6$). This can be explained by the replenishment of these compounds in the bacteria-containing droplets upon uptake from the gas phase and evaporation from the bacteria-free droplets, in which less efficient consumption of the organics occurs. Less soluble organics ($K_H < 10^4$ M atm^{-1}) that partition to a smaller extent (< 1%) to the aqueous phase are mostly consumed by chemical processes in the gas phase; more soluble compounds ($K_H > 10^6$ M atm^{-1}) are predominately partitioned to the aqueous phase and, thus, the evaporation to the gas phase and consequently the redistribution from the bacteria-free to the bacteria-containing droplets is kinetically more limited and less efficient. The ratio of the consumption of water-soluble organic gases by bacteria to the total loss (L_{bact}/L_t) might be as high as 0.7 for high biological activity and cell concentrations (~ 10^8 cells L^{-1}). These values suggest that biological processes might add significantly (>70%) to the loss processes in the atmospheric multiphase system for organics with intermediate solubility such as formic acid/formate, acetic acid/acetate or phenol. For CCN-derived compounds, the amount of organics consumed by bacteria is restricted to the fraction of the organic dissolved in bacteria-containing droplets (~ 0.001%) as no efficient replenishment from the gas phase or from the other droplets occurs. Thus, biodegradation of CCN-derived compounds does not significantly affect their atmospheric budget. Recent experiments of airborne bacteria suggested that metabolic rates are a function of substrate availability in oligotrophic media such as cloud droplets (Krumins et al., 2014b). In the case of CCN-derived organics or those that are inefficiently replenished by uptake from the gas phase, substrate limitation might result in lower biodegradation rates. Currently, no data is available on the absolute changes in k_{bact} at different levels of substrate availability and/or on the time scales during which k_{bact} might adjust to such conditions. In addition, the biodegradation rates may be affected under highly acidic conditions. Some studies demonstrated that some bacteria can develop an acid resistance to survive under acidic conditions (Lu et al., 2013). However, these strategies do not necessarily imply that the bacteria maintain the same biodegradation activities at high acidity but they allow survival of the cells in the atmosphere. It can be expected that internal buffering of bacteria cells allows them to maintain their metabolic activity over wide pH ranges (~3 to 6) as found in cloud water. Therefore, we do not consider a potential pH dependency of biodegradation rates in our model studies.

In addition to our detailed model with a realistic bacteria cell distribution within a cloud droplet population, we apply simpler model approaches: (i) Similar to many chemical model studies, bacteria cells are distributed equally in all droplets ('bulk approach') resulting in cell concentrations of 10^{-5} cells per droplet, clearly an unphysical assumption for intact bacteria cells. (ii) A multiphase system with only cloud droplets

which contain bacteria resulting in a liquid water content of ~10^{-11} vol/vol as compared to ~10^{-7} vol/vol in clouds ('low LWC approach'). Comparing L_{bact} predicted from these approaches to results of our detailed model shows that all approaches agree in predicting L_{bact} for organics of low solubility ($K_{H(eff)} < 10^4$ M atm^{-1}). However, for such species the importance of biodegradation is low due to their inefficient partitioning to the aqueous phase. The bulk approach increasingly overestimates L_{bact} of organics with higher K_H; the greatest discrepancy is predicted for highly soluble compounds ($K_{H(eff)} > 10^6$ M atm^{-1}) as the bulk approach does not take into account the kinetic limitation due to the organic redistribution between the bacteria-free and bacteria-containing droplets. As the bulk approach implies organics in all droplets, it does not allow limiting the organic consumption by biodegradation. Predictions of the relative role of biodegradation as compared to chemical processes by the 'low-LWC approach' are biased high because the loss due to aqueous phase processes is only considered in an unrealistically small fraction of droplets.

The current data sets for microbial rates of organic compounds are limited to very few compounds. Our model sensitivity study shows that biodegradation by bacteria in clouds is most efficient for compounds with intermediate (effective) Henry's law constants (~10^4 M atm^{-1} < $K_{H(eff)}$ < 10^6 M atm^{-1}) as found for common cloud water constituents such as formic acid/formate and acetic acid/acetate but also for less abundant species such as phenol, largely independent of their chemical reactivity. Our framework allows to estimate the potential importance of biodegradation of organics, in comparison to chemical processes. It also gives guidance to future lab and model studies to further explore the role of biodegradation of specific organics in the multiphase system.

Data availability: All model input data are summarized in Tables S1-S3 in the supplemental information.

Author contributions: AK and BE designed and carried out the model studies and wrote the manuscript. MZ, PA, AMD contributed by fruitful discussions and gave constructive feedback on the manuscript.

Competing interests: The authors declare no competing interests.

References

Allou, L., El Maimouni, L. and Le Calvé, S.: Henry's law constant measurements for formaldehyde and benzaldehyde as a function of temperature and water composition, Atmos. Environ., 45(17), 2991--2998, doi:10.1016/j.atmosenv.2010.05.044, 2011.

Amato, P., Demeer, F., Melaouhi, A., Fontanella, S., Martin-Biesse, A.-S., Sancelme, M., Laj, P. and Delort, A.-M.: A fate for organic acids, formaldehyde and methanol in cloud water: their biotransformation by micro-organisms, Atmos. Chem. Phys., 7(15), 4159–4169, doi:10.5194/acp-7-4159-2007, 2007a.

Amato, P., Demeer, F., Melaouhi, A., Fontanella, S., Martin-Biesse, A. S., Sancelme, M., Laj, P. and Delort, A. M.: A fate for organic acids, formaldehyde and methanol in cloud water: Their biotransformation by micro-organisms, Atmos. Chem. Phys., 7(2), 5253–5276, doi:10.5194/acp-7-4159-2007, 2007b.

Amato, P., Parazols, M., Sancelme, M., Mailhot, G., Laj, P. and Delort, A. M.: An important oceanic source of micro-organisms for cloud water at the Puy de Dôme (France), Atmos. Environ., 41(37), 8253–8263, doi:10.1016/j.atmosenv.2007.06.022, 2007c.

Amato, P., Parazols, M., Sancelme, M., Laj, P., Mailhot, G. and Delort, A. M.: Microorganisms isolated from the water phase of tropospheric clouds at the Puy de Dôme: Major groups and growth abilities at low temperatures, FEMS Microbiol. Ecol., 59(2), 242–254, doi:10.1111/j.1574-6941.2006.00199.x, 2007d.

Amato, P., Besaury, L., Joly, M., Penaud, B., Deguillaume, L. and Delort, A. M.: Metatranscriptomic exploration of microbial functioning in clouds, Sci. Rep., 9(1), 1–12, doi:10.1038/s41598-019-41032-4, 2019.

Anglada, J. M.: Complex mechanism of the gas phase reaction between formic acid and hydroxyl radical. Proton coupled electron transfer versus radical hydrogen abstraction mechanisms, J. Am. Chem. Soc., 126(31), 9809--9820, doi:10.1021/ja0481169, 2004.

Arakaki, T., Anastasio, C., Kuroki, Y., Nakajima, H., Okada, K., Kotani, Y., Handa, D., Azechi, S., Kimura, T., Tsuhako, A. and Miyagi, Y.: A general scavenging rate constant for reaction of hydroxyl radical with organic carbon in atmospheric waters, Environ. Sci. Technol., 47(15), 8196--8203, doi:10.1021/es401927b, 2013.

Ariya, P. A., Nepotchatykh, O., Ignatova, O. and Amyot, M.: Microbiological degradation of atmospheric organic compounds, Geophys. Res. Lett., 29(22), 34–1, doi:10.1029/2002gl015637, 2002.

Aumont, B., Madronich, S., Bey, I. and Tyndall, G.: Contribution of Secondary VOC to the Composition of Aqueous Atmospheric Particles: A Modeling Approach, J. Atmos. Chem., 35(1), 59–75, doi:10.1023/a:1006243509840, 2000.

Beard, K. V. and Ochs, H. T.: Collection and coalescence efficiencies for accretion., J. Geophys. Res., 89(D5), 7165–7169, doi:10.1029/JD089iD05p07165, 1984.

Butkovskaya, N. I., Kukui, A., Pouvesle, N. and Le Bras, G.: Rate constant and mechanism of the reaction of OH radicals with acetic acid in the temperature range of 229-300 K, J. Phys. Chem. A, 108(34), 7021--7026, doi:10.1021/jp048444v, 2004.

Cabelli, Diane E and Bielski, B. H.: pulse radiolysis study of some dicarboxylic acids of the citric acid cycle. The kinetics and spectral properties of the free radicals formed by reactions with the HO radical, Zeitschrift für Naturforsch. B, 40(12), 1731--1737, doi:https://doi.org/10.1515/znb-1985-1223, 1985.

Cantrell, C. A., Shetter, R. E., Calvert, J. G., Eisele, F. L. and Tanner, D. J.: Some considerations of the origin of nighttime peroxy radicals observed in MLOPEX 2c, J. Geophys. Res. Atmos., 102(D13), 15899--

675 15913, doi:10.1029/97jd01120, 1997.

Decesari, S., Facchini, M. C., Fuzzi, S. and Tagliavini, E.: Characterization of water-soluble organic compounds in atmospheric aerosol: A new approach, J. Geophys. Res. Atmos., 105(D1), 1481–1489, doi:10.1029/1999JD900950, 2000.

Deguillaume, L., Charbouillot, T., Joly, M., Vaïtilingom, M., Parazols, M., Marinoni, A., Amato, P., Delort,
680 A. M., Vinatier, V., Flossmann, A., Chaumerliac, N., Pichon, J. M., Houdier, S., Laj, P., Sellegri, K., Colomb, A., Brigante, M. and Mailhot, G.: Classification of clouds sampled at the puy de Dôme (France) based on 10 yr of monitoring of their physicochemical properties, Atmos. Chem. Phys., doi:10.5194/acp-14-1485-2014, 2014.

Delort, A.-M., Deguillaume, L., Renard, P., Vinatier, V., Canet, I., Vaïtilingom, M. and Chaumerliac, N.:
685 Impacts on Cloud Chemistry, in Microbiology of Aerosols., 2017.

Delort, A. M., Vaïtilingom, M., Amato, P., Sancelme, M., Parazols, M., Mailhot, G., Laj, P. and Deguillaume, L.: A short overview of the microbial population in clouds: Potential roles in atmospheric chemistry and nucleation processes, Atmos. Res., 98(2–4), 249–260, doi:10.1016/j.atmosres.2010.07.004, 2010.

690 Ervens, B.: Modeling the Processing of Aerosol and Trace Gases in Clouds and Fogs, Chem. Rev., 115(10), 4157--4198, doi:10.1021/cr5005887, 2015.

Ervens, B. and Amato, P.: The global impact of bacterial processes on carbon mass, Atmos. Chem. Physics& Phys., 20(3), doi:10.5194/acp-20-1777-2020, 2020.

Ervens, B., George, C., Williams, J. E., Buxton, G. V., Salmon, G. A., Bydder, M., Wilkinson, F., Dentener,
695 F., Mirabel, P., Wolke, R. and Herrmann, H.: CAPRAM 2.4 (MODAC mechanism): An extended and condensed tropospheric aqueous phase mechanism and its application, J. Geophys. Res. Atmos., 108(D14), doi:10.1029/2002jd002202, 2003a.

Ervens, B., Herckes, P., Feingold, G., Lee, T., Collett, J. L. and Kreidenweis, S. M.: On the drop-size dependence of organic acid and formaldehyde concentrations in fog, J. Atmos. Chem., 46(3), 239–269,
700 doi:10.1023/A:1026393805907, 2003b.

Ervens, B., Gligorovski, S. and Herrmann, H.: Temperature-dependent rate constants for hydroxyl radical reactions with organic compounds in aqueous solutions, Phys. Chem. Chem. Phys., 5(9), 1811–1824, doi:10.1039/b300072a, 2003c.

Ervens, B., Feingold, G., Frost, G. J. and Kreidenweis, S. M.: A modeling of study of aqueous production
705 of dicarboxylic acids: 1. Chemical pathways and speciated organic mass production, J. Geophys. Res. D Atmos., 109(D15), doi:10.1029/2003JD004387, 2004.

Ervens, B., Carlton, A. G., Turpin, B. J., Altieri, K. E., Kreidenweis, S. M. and Feingold, G.: Secondary organic aerosol yields from cloud-processing of isoprene oxidation products, Geophys. Res. Lett., 35(2),

doi:10.1029/2007GL031828, 2008.

710   Exner, M., Herrmann, H. and Zellner, R.: Rate constants for the reactions of the NO3 radical with HCOOH/HCOO- and CH3COOH/CH3COO- in aqueous solution between 278 and 328 K, J. Atmos. Chem., 18(4), 359--378, doi:10.1007/BF00712451, 1994.

Fankhauser, A. M., Antonio, D. D., Krell, A., Alston, S. J., Banta, S. and McNeill, V. F.: Constraining the Impact of Bacteria on the Aqueous Atmospheric Chemistry of Small Organic Compounds, ACS Earth Sp.

715   Chem., 3(8), 1485–1491, doi:10.1021/acsearthspacechem.9b00054, 2019.

Fu, P., Kawamura, K., Usukura, K. and Miura, K.: Dicarboxylic acids, ketocarboxylic acids and glyoxal in the marine aerosols collected during a round-the-world cruise, Mar. Chem., 148, 22–32, doi:10.1016/j.marchem.2012.11.002, 2013.

Gaillard De Sémainville, P., Hoffmann, D., George, C. and Herrmann, H.: Study of nitrate radical (NO3)

720   reactions with carbonyls and acids in aqueous solution as a function of temperature, Phys. Chem. Chem. Phys., 9(8), 958--968, doi:10.1039/b613956f, 2007.

Gao, Y., Lee, S. C., Huang, Y., Chow, J. C. and Watson, J. G.: Chemical characterization and source apportionment of size-resolved particles in Hong Kong sub-urban area, Atmos. Res., 170, 112–122, doi:10.1016/j.atmosres.2015.11.015, 2016.

725   Guan, N. and Liu, L.: Microbial response to acid stress: mechanisms and applications, Appl. Microbiol. Biotechnol., 51–65, doi:10.1007/s00253-019-10226-1, 2020.

Haddrell, A. E. and Thomas, R. J.: Aerobiology: Experimental considerations, observations, and future tools, Appl. Environ. Microbiol., 83(17), doi:10.1128/AEM.00809-17, 2017.

Herckes, P., Valsaraj, K. T. and Collett, J. L.: A review of observations of organic matter in fogs and clouds:

730   Origin, processing and fate, Atmos. Res., 434–449, doi:10.1016/j.atmosres.2013.06.005, 2013.

Herlihy, L. J., Galloway, J. N. and Mills, A. L.: Bacterial utilization of formic and acetic acid in rainwater, Atmos. Environ., 21(11), 2397–2402, doi:10.1016/0004-6981(87)90374-X, 1987.

Herrmann, H.: Kinetics of Aqueous Phase Reactions Relevant for Atmospheric Chemistry, Chem. Rev., 103(12), 4691–4716, doi:10.1021/cr020658q, 2003.

735   Hoffmann, E. H., Tilgner, A., Wolke, R., Böge, O., Walter, A. and Herrmann, H.: Oxidation of substituted aromatic hydrocarbons in the tropospheric aqueous phase: Kinetic mechanism development and modelling, Phys. Chem. Chem. Phys., 20(16), 10960--10977, doi:10.1039/c7cp08576a, 2018.

Hu, W., Niu, H., Murata, K., Wu, Z., Hu, M., Kojima, T. and Zhang, D.: Bacteria in atmospheric waters: Detection, characteristics and implications, Atmos. Environ., 201–221,

740   doi:10.1016/j.atmosenv.2018.02.026, 2018.

Husárová, S., Vaïtilingom, M., Deguillaume, L., Traikia, M., Vinatier, V., Sancelme, M., Amato, P., Matulová, M. and Delort, A. M.: Biotransformation of methanol and formaldehyde by bacteria isolated from

clouds. Comparison with radical chemistry, Atmos. Environ., 45(33), 6093–6102, doi:10.1016/j.atmosenv.2011.06.035, 2011.

745   Jaber, S., Lallement, A., Sancelme, M., Leremboure, M., Mailhot, G., Ervens, B. and Delort, A.-M.: Biodegradation of phenol and catechol in cloud water: Comparison to chemical oxidation in the atmospheric multiphase system, Atmos. Chem. Phys. Discuss., 20(8), doi:10.5194/acp-2019-1048, 2020.

Jacob, D. J.: Chemistry of OH in remote clouds and its role in the production of formic acid and peroxymonosulfate, J. Geophys. Res., 91(D9), 9807--9826, doi:10.1029/jd091id09p09807, 1986.

750   Johnson, B. J., Betterton, E. A. and Craig, D.: Henry's Law coefficients of formic and acetic acids, J. Atmos. Chem., 24(2), 113--119, doi:10.1007/BF00162406, 1996.

Kaprelyants, A. S. and Kell, D. B.: Dormancy in stationary-phase cultures of Micrococcus luteus: Flow cytometric analysis of starvation and resuscitation, Appl. Environ. Microbiol., 59(10), 3187–3196, doi:10.1128/aem.59.10.3187-3196.1993, 1993.

755   Kawamura, K. and Ikushima, K.: Seasonal Changes in the Distribution of Dicarboxylic Acids in the Urban Atmosphere, Environ. Sci. Technol., 27(10), 2227–2235, doi:10.1021/es00047a033, 1993.

Khan, M. A. H., Ashfold, M. J., Nickless, G., Martin, D., Watson, L. A., Hamer, P. D., Wayne, R. P., Canosa-Mas, C. E. and Shallcross, D. E.: Night-time NO3 and OH radical concentrations in the United Kingdom inferred from hydrocarbon measurements, Atmos. Sci. Lett., 9(3), 140--146, doi:10.1002/asl.175,

760   2008.

Khare, P., Kumar, N., Kumari, K. M. and Srivastava, S. S.: Atmospheric formic and acetic acids: An overview, Rev. Geophys., 37(2), 227–248, doi:10.1029/1998RG900005, 1999.

Krumins, V., Mainelis, G., Kerkhof, L. J. and Fennell, D. E.: Substrate-Dependent rRNA Production in an Airborne Bacterium, Environ. Sci. Technol. Lett., 1(9), 376–381, doi:10.1021/ez500245y, 2014a.

765   Krumins, V., Mainelis, G., Kerkhof, L. J. and Fennell, D. E.: Substrate-Dependent rRNA Production in an Airborne Bacterium, Environ. Sci. Technol. Lett., 1(9), 376–381, doi:10.1021/ez500245y, 2014b.

Lelieveld, J. and Crutzen, P. J.: The role of clouds in tropospheric photochemistry, J. Atmos. Chem., 12(3), 229–267, doi:10.1007/BF00048075, 1991.

Löflund, M., Kasper-Giebl, A., Schuster, B., Giebl, H., Hitzenberger, R. and Puxbaum, H.: Formic, acetic,

770   oxalic, malonic and succinic acid concentrations and their contribution to organic carbon in cloud water, Atmos. Environ., 36(9), 1553–1558, doi:10.1016/S1352-2310(01)00573-8, 2002.

Lu, P., Ma, D., Chen, Y., Guo, Y., Chen, G. Q., Deng, H. and Shi, Y.: L-glutamine provides acid resistance for Escherichia coli through enzymatic release of ammonia, Cell Res., doi:10.1038/cr.2013.13, 2013.

Madronich, S. and Calvert, J. G.: No Title, NCAR Tech. Note TN-474+STR, 1989.

775   Mezyk, S. P., Cullen, T. D., Rickman, K. A. and Mincher, B. J.: The Reactivity of the Nitrate Radical (•NO3) in Aqueous and Organic Solutions, Int. J. Chem. Kinet., 49(9), 635--642, doi:10.1002/kin.21103, 2017.

Mouchel-Vallon, C., Deguillaume, L., Monod, A., Perroux, H., Rose, C., Ghigo, G., Long, Y., Leriche, M., Aumont, B., Patryl, L., Armand, P. and Chaumerliac, N.: CLEPS 1.0: A new protocol for cloud aqueous phase oxidation of VOC mechanisms, Geosci. Model Dev., 10(3), 1339–1362, doi:10.5194/gmd-10-1339-2017, 2017.

Pillar, E. A., Camm, R. C. and Guzman, M. I.: Catechol oxidation by ozone and hydroxyl radicals at the air-water interface, Environ. Sci. Technol., 48(24), 14352–14360, doi:10.1021/es504094x, 2014.

Razika, B., Abbes, B., Messaoud, C. and Soufi, K.: Phenol and Benzoic Acid Degradation by Pseudomonas aeruginosa, J. Water Resour. Prot., 2(9), 1–4, doi:10.4236/jwarp.2010.29092, 2010.

Sander, R.: Compilation of Henry's law constants (version 4.0) for water as solvent, Atmos. Chem. Phys., 15(8), 4399–4981, doi:10.5194/acp-15-4399-2015, 2015.

Sattler, B., Puxbaum, H. and Psenner, R.: Bacterial growth in supercooled cloud droplets, Geophys. Res. Lett., doi:10.1029/2000GL011684, 2001.

Schwartz, S. E.: Mass-Transport Considerations Pertinent to Aqueous Phase Reactions of Gases in Liquid-Water Clouds, in Chemistry of Multiphase Atmospheric Systems, pp. 415–471., 1986.

Seinfeld, J. H. and Pandis, S. N.: Atmospheric Chemistry and Physics, John Wiley & Sons, New York., 1998.

Sun, X., Wang, Y., Li, H., Yang, X., Sun, L., Wang, X., Wang, T. and Wang, W.: Organic acids in cloud water and rainwater at a mountain site in acid rain areas of South China, Environ. Sci. Pollut. Res., 23(10), 9529–9539, doi:10.1007/s11356-016-6038-1, 2016.

Tilgner, A., Bräuer, P., Wolke, R. and Herrmann, H.: Modelling multiphase chemistry in deliquescent aerosols and clouds using CAPRAM3.0i, J. Atmos. Chem., 70(3), 221–256, doi:10.1007/s10874-013-9267-4, 2013.

Vaïtilingom, M., Amato, P., Sancelme, M., Laj, P., Leriche, M. and Delort, A. M.: Contribution of microbial activity to carbon chemistry in clouds, Appl. Environ. Microbiol., 76(1), 23–29, doi:10.1128/AEM.01127-09, 2010a.

Vaïtilingom, M., Amato, P., Sancelme, M., Laj, P., Leriche, M. and Delort, A.-M.: Contribution of Microbial Activity to Carbon Chemistry in Clouds, Appl. Environ. Microbiol., 76(1), 23–29, doi:10.1128/AEM.01127-09, 2010b.

Vaïtilingom, M., Charbouillot, T., Deguillaume, L., Maisonobe, R., Parazols, M., Amato, P., Sancelme, M. and Delort, A. M.: Atmospheric chemistry of carboxylic acids: Microbial implication versus photochemistry, Atmos. Chem. Phys., 11(2), 4881–4911, doi:10.5194/acp-11-8721-2011, 2011.

Vaïtilingom, M., Deguillaume, L., Vinatier, V., Sancelme, M., Amato, P., Chaumerliac, N. and Delort, A.-M.: Potential impact of microbial activity on the oxidant capacity and organic carbon budget in clouds, Proc. Natl. Acad. Sci., 110(2), 559–564, doi:10.1073/pnas.1205743110, 2013a.

Vaïtilingom, M., Deguillaume, L., Vinatier, V., Sancelme, M., Amato, P., Chaumerliac, N. and Delort, A. M.: Potential impact of microbial activity on the oxidant capacity and organic carbon budget in clouds, Proc. Natl. Acad. Sci. U. S. A., 110(2), 559–564, doi:10.1073/pnas.1205743110, 2013b.

Varga, B., Kiss, G., Ganszky, I., Gelencsér, A. and Krivácsy, Z.: Isolation of water-soluble organic matter from atmospheric aerosol, Talanta, 55(3), 561–572, doi:10.1016/S0039-9140(01)00446-5, 2001.

Woo, J. L. and McNeill, V. F.: simpleGAMMA v1.0 - A reduced model of secondary organic aerosol formation in the aqueous aerosol phase (aaSOA), Geosci. Model Dev., 8(6), 1821, doi:10.5194/gmd-8-1821-2015, 2015.

Zhang, M., Khaled, A., Amato, P., Delort, A. and Ervens, B.: the effect of biological particles and their ageing processes on aerosol radiative properties: Model sensitivity studies, Atmos. Chem. Phys. Submitt., 2020.

825